~~Protoplanetary and circumstellar disks~~

~~Turbulent accretion disks~~

~~Cold and hot disks~~

~~Optically thick disks~~

~~Disks: dynamics & observations~~

~~Radiation transfer in whatever disks~~

Disks ← why?

Miroslav Brož, in collaboration w. Ondřej Chrenko, David Nesvorný, Jana Nemravová,
Denis Mourard, Petr Harmanec, ...

Evolution of 3-Earth-mass protoplanets towards eventual gap opening

or so...

Miroslav Brož[1], Ondřej Chrenko[1], David Nesvorný[2] - [1]Charles University in Prague, V Holešovičkách 2, 18000 Prague, Czech Republic; [2]SWRI - email: mira@sirrah.troja.mff.cuni.cz

Abstract: Several-Earth-mass protoplanets interact with the gaseous and pebble disk in a complex way (see Chrenko et al. 2017, or Eklund & Masset 2017). The **hot-trail effect** arises as a consequence of accretion heating, it raises planetary eccentricities, and may prevent resonant captures of migrating planets. Here we study the dependence of this effect on parameters such as the surface density, viscosity, or the number of protoplanets. After mergers, planets are massive enough to accrete massive gas envelopes, open gaps, and eventually Type-I migration changes to Type-II. We are also using hydrocode results and radiation transfer code to compute how disk would appear in ALMA observations and whether this may constrain the properties of embedded planets.

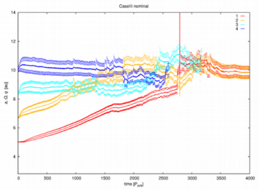

CaseIII_nominal — As presented in Chrenko et al. (2017). Starting with 4 embryos, 3 M_E, initial spacing 10 R_{Hill}, pebble flux 2×10^{-4} M_E per yr, approx. MMSN, with 0.5 $\Sigma(r)$ slope, kinematic viscosity $\nu = 10^{-5}$ [c.u.], proto-Sun, resolution 1024×1536, damping BC's, artificial inclination damping (Tanaka & Ward 2004), no Hill cut. Results: hot-trail effect, high eccentricities (cf. talk by O. Chrenko), 0-torque at approx. 9 au, no low-order mean-motion resonances (MMR), because embryos were too close, capture difficult anyway (because $e > 0$), two successful mergers 13.8 M_E and 4.3 M_E, but co-orbitals, their long-term evolution? We performed 6 additional simulations, always with a single modified parameter...

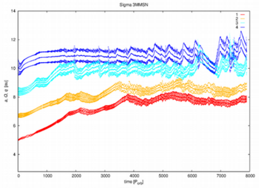

Sigma_3MMSN — initial surface density Σ 3× larger; 0-torque radius further out at 11 au, e often *smaller*, slower evolution (even though timespan 2× longer), embryos do NOT interact so strongly, rather stay next to each other, because damping is too large? sometimes inward migration of inner embryos @ larger e, possible interference of (massive) co-orbital regions? 10+ attempts of the outer 4th embryo to enter the co-orbital region of the 3rd one, only temporary coorbitals.

any comments? write them here!

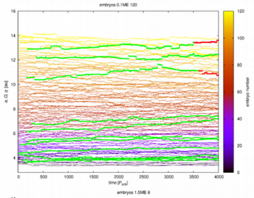

embryos_0.1ME_120 — 120 low-mass 0.1 M_E embryos, spacing 2 mutual R_{Hill}, disk up to 16 au, resolution still low (3 pixels per Hill sphere), at least 2048×3072 would be needed, convergence tests show that da/dt is *overestimated*, very slow computation anyway (120 disk → planet interactions), it was run on Pleiades, caveat: collisional radii increased only during merger events; overlapping weak spiral arms, slow evolution dominated by encounters, e up to 0.06, 10+ quick mergers 0.2 M_E, pebble accretion up to 0.45 M_E, but strong filtering for inner embryos, 0.2 M_E mergers are either inside (short periods) or outside, the "winner" is outside (no filtering), longer simulation needed?

any comments?

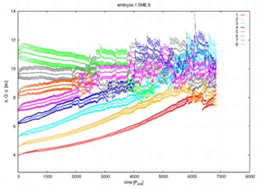

embryos_1.5ME_8 — 8 embryos with 1.5 M_E, clear convergence to 0-torque, slower evolution, a number of encounters, more opportunities to merge, especially when an additional embryo arrives and starts to interact, 2 mergers 13.2 and 6.5 M_E as of yet, more outer embryos should be added and an extended disk (20 au) should be used?

any comments?

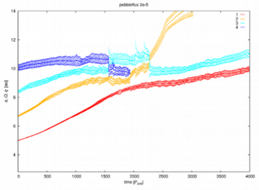

pebbleflux_2e-5 — 10× lower pebble flux 2×10^{-5} M_E, i.e. 0.25 M_E per 4000 P_{orb} (more realistic?), lower eccentricity excitation (!), consequently smooth evolution, all embryos initially drift outwards, 0-torque at about 11 au? 1 yellow merger with 6 M_E quickly drifts outwards (!), only temporarily decelerated by the 3rd embryo, *runaway* migration mode as in Pierens & Raymond (2016)? planet IX? :) Is it a rule for low pebble fluxes? Possible clearing of the outer disk? More outer embryos should be probably added...

any comments?

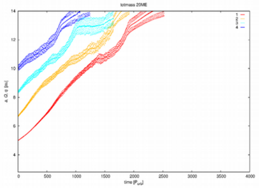

totmass_20ME — initial masses 5 M_E; all embryos quickly drift outwards (!), even though wo. heating the 0-torque should be at 7 au; lower e, practically NO interactions, because real 0-torque is further out, unwanted interactions with the disk edge; larger disk & more embryos shoud be used...

any comments?

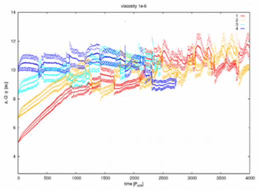

viscosity_1e-6 — low-viscosity disk; same e, BUT faster migration da/dt, i.e. like ν in the denominator (?!), surroundings more easily affected by the embryo, many encounters, only temporary co-orbitals, 2 mergers 8 M_E as of yet, an onset of gap opening even without gas-accretion term? many attempts to form a co-orbital pair, BUT failed co-orbital formation? (cf. Figs. above)

any comments?

$$\frac{\partial\Sigma}{\partial t} + \overbrace{\boldsymbol{v}\cdot\nabla\Sigma}^{\text{convection}} = -\overbrace{\Sigma\nabla\cdot\boldsymbol{v}}^{\text{expansion}} - \overbrace{\left(\frac{\partial\Sigma}{\partial t}\right)_{\text{acc}}}^{\text{gas accretion}}$$

$$\frac{\partial\boldsymbol{v}}{\partial t} + \boldsymbol{v}\cdot\nabla\boldsymbol{v} = -\frac{1}{\Sigma}\nabla P + \overbrace{\frac{1}{\Sigma}\nabla\cdot\mathsf{T}}^{\text{bulk viscosity}} - \overbrace{\frac{\int\rho\nabla\phi\,\mathrm{d}z}{\Sigma}}^{\text{gravity}} + \overbrace{\frac{\Sigma_{\text{p}}}{\Sigma}\frac{\Omega_{\text{K}}}{\tau}(\boldsymbol{u}-\boldsymbol{v})}^{\text{back-reaction}}$$

$$\frac{\partial E}{\partial t} + \boldsymbol{v}\cdot\nabla E = -E\nabla\cdot\boldsymbol{v} - P\nabla\cdot\boldsymbol{v} + \overbrace{Q_{\text{visc}}}^{\text{dissip.}} + \overbrace{\frac{2\sigma T_{\text{irr}}^4}{\tau_{\text{eff}}}}^{\text{irradiation}} - \overbrace{\frac{2\sigma T^4}{\tau_{\text{eff}}}}^{\text{vertical cooling}} + \overbrace{2H\nabla\cdot\frac{16\sigma\lambda_{\text{lim}}}{\rho_0\kappa}T^3\nabla T}^{\text{radiative diffusion}} + \overbrace{\frac{GM\dot{M}}{RS_{\text{cell}}}}^{\text{accretion}}$$

$$\frac{\partial\Sigma_{\text{p}}}{\partial t} + \boldsymbol{u}\cdot\nabla\Sigma_{\text{p}} = -\Sigma_{\text{p}}\nabla\cdot\boldsymbol{u} - \overbrace{\left(\frac{\partial\Sigma_{\text{p}}}{\partial t}\right)_{\text{acc}}}^{\text{pebble accretion}}$$

$$\frac{\partial\boldsymbol{u}}{\partial t} + \boldsymbol{u}\cdot\nabla\boldsymbol{u} = -\frac{\int\rho_{\text{p}}\nabla\phi\,\mathrm{d}z}{\Sigma_{\text{p}}} - \overbrace{\frac{\Omega_{\text{K}}}{\tau}(\boldsymbol{u}-\boldsymbol{v})}^{\text{aerodynamic drag}}$$

$$P = \Sigma\frac{RT}{\mu} = (\gamma-1)E$$

System of equations; changes w.r.t. Chrenko et al. (2017): gas accretion (Kley's prescription for 3D orbits), corresponding gas-accretion heating, fragmentation-limited pebbles, improved SOR convergence.

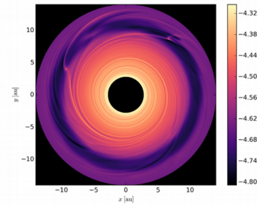

Figure: Evolved gas disk @ time $t = 4000$ P_{orb} @ 5.2 au, hot-trail effect visible, failed co-orbital, viscosity_1e-6.

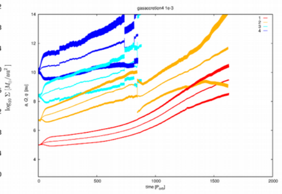

Figure: Simulation with gas accretion (incl. heating), Kley parameter $f_{acc} = 10^{-3}$, $\Delta M \propto f_{acc}\Sigma S_{cell}\Delta t \int\rho(z)\mathrm{d}z$.

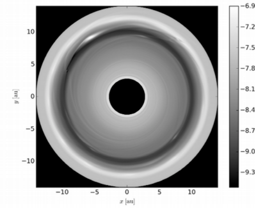

Figure: Pebble disk, corresponding 1:1 to the gas disk.

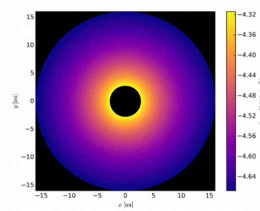

Figure: Gas disk with initially 120 embryos 0.1 M_E, and many weak overlapping spiral arms, $t = 4000$ P_{orb}.

Observability: The disk is optically thick in the vertical direction $\tau = \kappa\rho H \simeq 10^2 \gg 1$, with Bell & Lin (1994) integral opacities. It is thus necessary to properly model the disk atmosphere. In the midplane, the mean-free path l_f of gas molecules is small enough to assure a sufficient thermal contact and equilibrium between the gas and dust. This is no more true far from the midplane and one has to use 3D, non-equilibrium model, and monochromatic opacities (cf. eqs.). While surface-area distribution of solids is dominated by sub-micron dust, the mass distribution is dominated by pebbles (as in Birnstiel et al. 2012); in principle we can use Σ_p, $H_p < H$, $\kappa_p \ll \kappa$, but it could hardly produce observable effects.

We tried to use Radmc-3D code (Dullemond et al. 2012), assuming LTE, dust absorption, isotropic scattering, central star, possibly also embryos heated by pebble accretion, and viscous heating (i.e. an extended source). Synthetic image for 10^8 photons was processed by ALMA OST, assuming high $\nu = 900$ GHz, 7.5 GHz bandwidth, 3-hour observation, 1 visit starting at 78°, PWV 0.475 mm, and extended (full) configuration with baselines up to $B/\lambda = 3.6\times10^6$ cycles.

Problems: (i) only fully-opened gaps seem observable; (ii) only escape-probability, no Λ-iterations, ALI, or Ng-acceleration → a slow convergence with extended source inside optically-thick disk interior!

$$\Sigma_{\text{d}} = \Sigma\,\kappa\,\frac{\int_\nu \frac{1}{\kappa_\nu}\frac{\mathrm{d}B_\nu}{\mathrm{d}T}\mathrm{d}\nu}{\int_\nu \frac{\mathrm{d}B_\nu}{\mathrm{d}T}\mathrm{d}\nu}$$

$$\rho_{\text{d}} = \frac{\Sigma_{\text{d}}}{\sqrt{2\pi}H}\exp\left(-\frac{z^2}{2H^2}\right)$$

$$\frac{\mathrm{d}I_\nu}{\mathrm{d}s} = \kappa_\nu^{\text{abs}}\rho B_\nu(T) + \frac{\kappa_\nu^{\text{sca}}\rho}{4\pi}\int I_\nu\mathrm{d}\Omega - (\kappa_\nu^{\text{abs}}+\kappa_\nu^{\text{sca}})\rho I_\nu$$

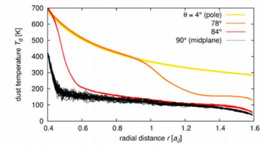

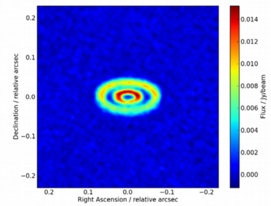

Conclusions:

Clearly, the dependence on parameters is complex! Apart from the very origin of gas-giant cores, there are a number of possible applications here: studies of different parts of the disk, origin of Uranus & Neptune, dynamics of other (compact) planetary systems. However, we have to face several serious problems: (i) find BC's suitable for the inner disk edge; (ii) resolve different pebble isolation in 2D vs 3D; (iii) gas accretion in 2D is not self-consistent, produces too much heating. It's possible that the deposition is below opaque atmosphere. A parametrisation of 3D in- and *outflows* (Lambrechts & Lega 2017) would be needed for this purpose.

Btw. the code is available @ http://sirrah.troja.mff.cuni.cz/~chrenko/

References:

Bell & Lin (1994) ApJ, **768**, 35
Birnstiel et al. (2012) A&A, **539**, A148
Chrenko et al. (2017) A&A, in press
Crida & Bitsch (2017) Icarus, **285**, 145
Dullemond et al. (2012) ASCL, 1202.015
Eklund & Masset (2017) MNRAS, **469**, 206
Lambrechts & Lega (2017) A&A, in press
Pierens & Raymond (2016) MNRAS, **462**, 4130
Tanaka & Ward (2004) ApJ, **602**, 388

1 slide

Q: How to compute a(t)? of planets

- mutual gravity (N-body)
- tides, spin-orbit coupling, relativistic precession, ...
- disk gravity, spiral arms, Lindblad torque (HD) ←
- corotation region, c. torque →
- cold finger (RHD) →→
- hot trail (in *e*) ←

⋮

$$\frac{\partial \Sigma}{\partial t} + \overbrace{\boldsymbol{v} \cdot \nabla \Sigma}^{\text{convection}} = - \overbrace{\Sigma \nabla \cdot \boldsymbol{v}}^{\text{expansion}} - \overbrace{\left(\frac{\partial \Sigma}{\partial t}\right)_{\text{acc}}}^{\text{gas accretion}}$$

$$\frac{\partial \boldsymbol{v}}{\partial t} + \boldsymbol{v} \cdot \nabla \boldsymbol{v} = -\frac{1}{\Sigma}\nabla P + \overbrace{\frac{1}{\Sigma}\nabla \cdot \mathsf{T}}^{\text{bulk viscosity}} - \overbrace{\frac{\int \rho \nabla \phi \, \mathrm{d}z}{\Sigma}}^{\text{gravity}} + \overbrace{\frac{\Sigma_{\text{p}}}{\Sigma}\frac{\Omega_{\text{K}}}{\tau}(\boldsymbol{u} - \boldsymbol{v})}^{\text{back-reaction}}$$

$$\frac{\partial E}{\partial t} + \boldsymbol{v} \cdot \nabla E = -E \nabla \cdot \boldsymbol{v} - P \nabla \cdot \boldsymbol{v} + \overbrace{Q_{\text{visc}}}^{\text{dissip.}} + \overbrace{\frac{2\sigma T_{\text{irr}}^4}{\tau_{\text{eff}}}}^{\text{irradiation}} - \overbrace{\frac{2\sigma T^4}{\tau_{\text{eff}}}}^{\substack{\text{vertical}\\\text{cooling}}} + \overbrace{2H \nabla \cdot \frac{16\sigma \lambda_{\text{lim}}}{\rho_0 \kappa} T^3 \nabla T}^{\text{radiative diffusion}} + \overbrace{\frac{GM\dot{M}}{RS_{\text{cell}}}}^{\text{accretion}}$$

$$\frac{\partial \Sigma_{\text{p}}}{\partial t} + \boldsymbol{u} \cdot \nabla \Sigma_{\text{p}} = -\Sigma_{\text{p}} \nabla \cdot \boldsymbol{u} - \overbrace{\left(\frac{\partial \Sigma_{\text{p}}}{\partial t}\right)_{\text{acc}}}^{\text{pebble accretion}}$$

$$\frac{\partial \boldsymbol{u}}{\partial t} + \boldsymbol{u} \cdot \nabla \boldsymbol{u} = -\frac{\int \rho_{\text{p}} \nabla \phi \, \mathrm{d}z}{\Sigma_{\text{p}}} - \overbrace{\frac{\Omega_{\text{K}}}{\tau}(\boldsymbol{u} - \boldsymbol{v})}^{\text{aerodynamic drag}}$$

$$P = \Sigma \frac{RT}{\mu} = (\gamma - 1)E$$

RHD
FMT
BC
IC?

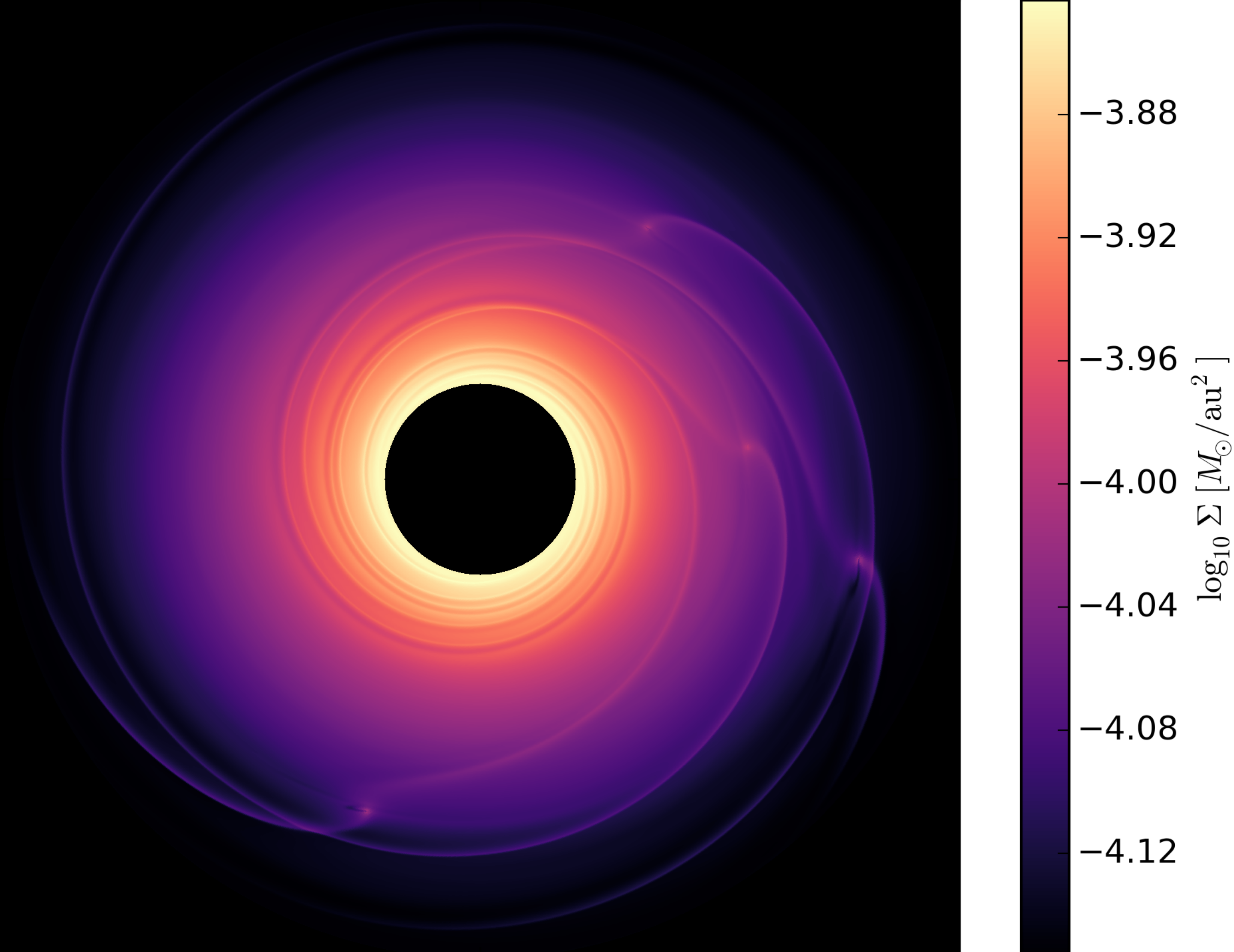

−3.88
−3.92
−3.96
−4.00
−4.04
−4.08
−4.12
$\log_{10} \Sigma \, [M_\odot/\mathrm{au}^2]$

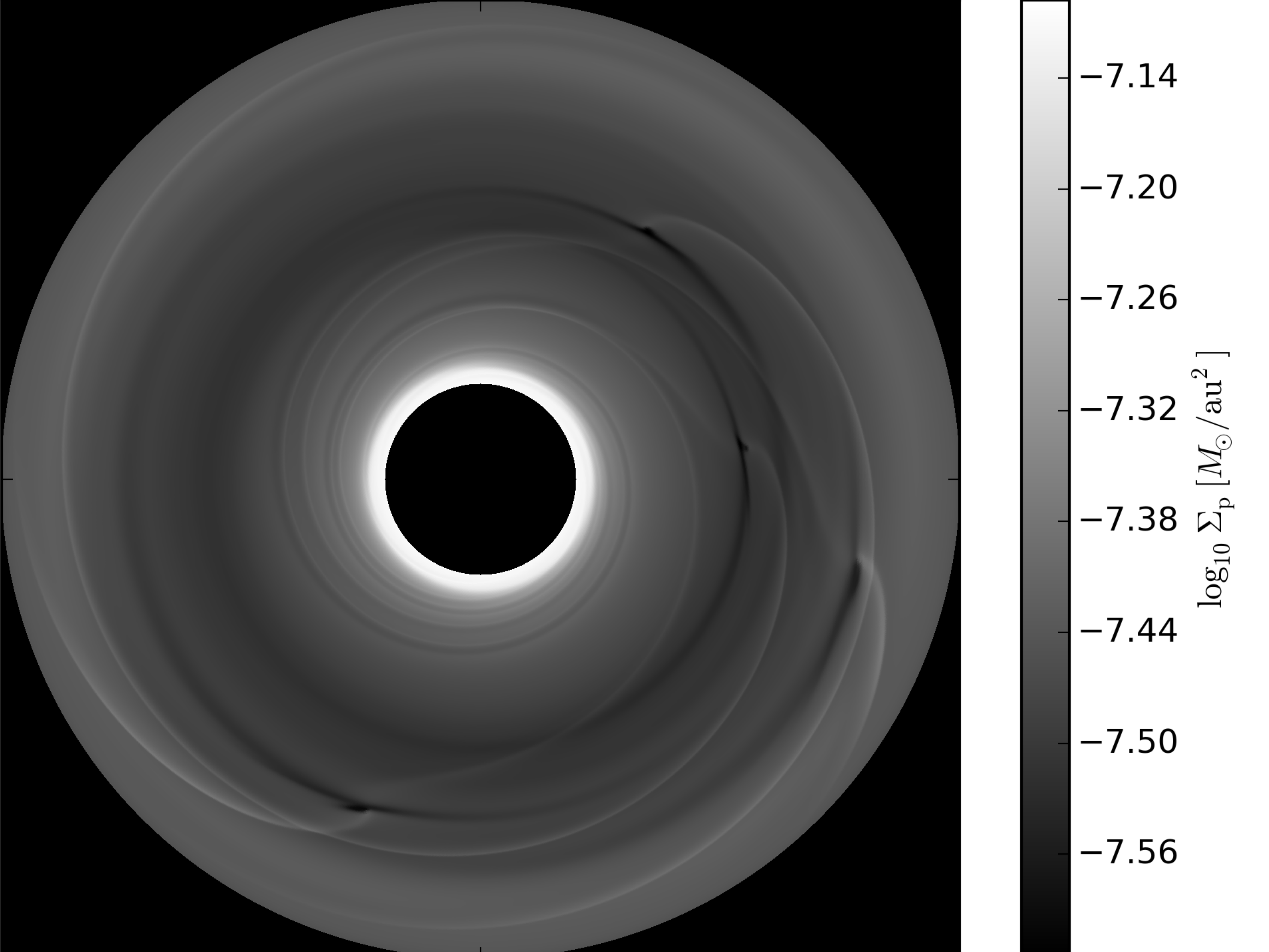
−7.14
−7.20
−7.26
−7.32
−7.38
−7.44
−7.50
−7.56
$\log_{10}\Sigma_{\rm p}\,[M_\odot/{\rm au}^2]$

Stellar-solar context

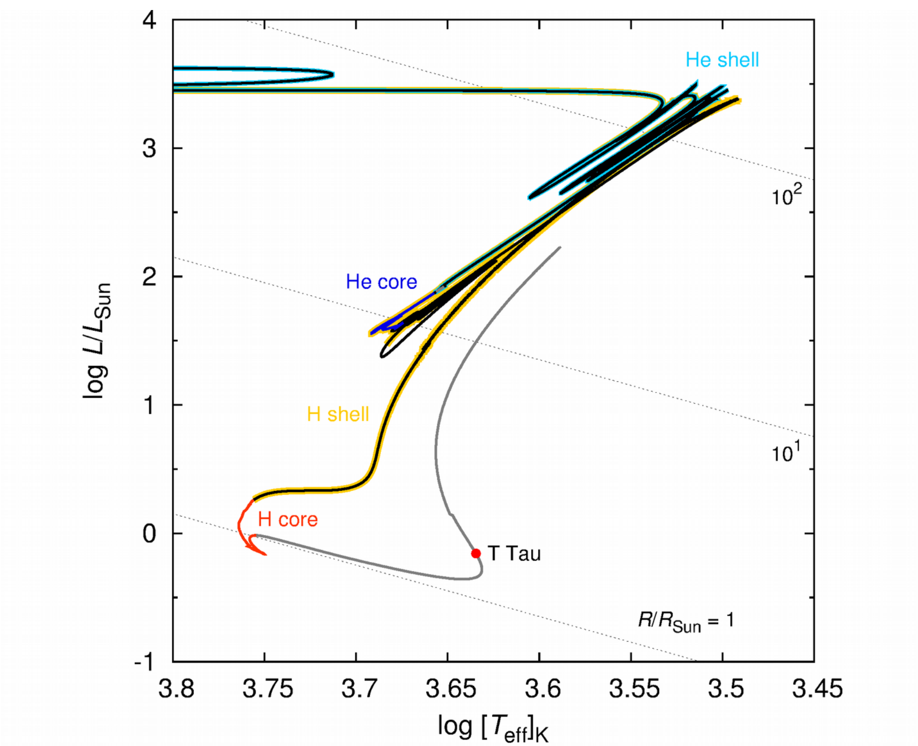

Fig. 1. The Hertzsprung–Russel diagram for a star (Sun) with the initial mass $M = 1\ M_{\odot}$, helium abundance $Y = 0.274$, metallicity $Z = 0.0195$, mixing length parameter $\alpha = 2.1$, Reimers RGB wind with the scaling factor $\eta_R = 0.6$, Blocker AGB wind with $\eta_B = 0.1$. The element diffision was also accounted for. Colours indicate four major burning phases: H core, H shell, He core and He shell burning. The red point denoted "T Tau" corresponds to the pre-main sequence object we use in our protoplanetary disk simulations. The evolution was calculated by Mesastar code, rev. 8845; Paxton et al. (2015).

- T Tauri (hydrostatic) phase
- receding convective zone (tachocline) && fast rotation (~2 d) → magnetic dynamo
- corotation cavity in the disk
- d. turbulence: VSI, SBI, MRI → ν

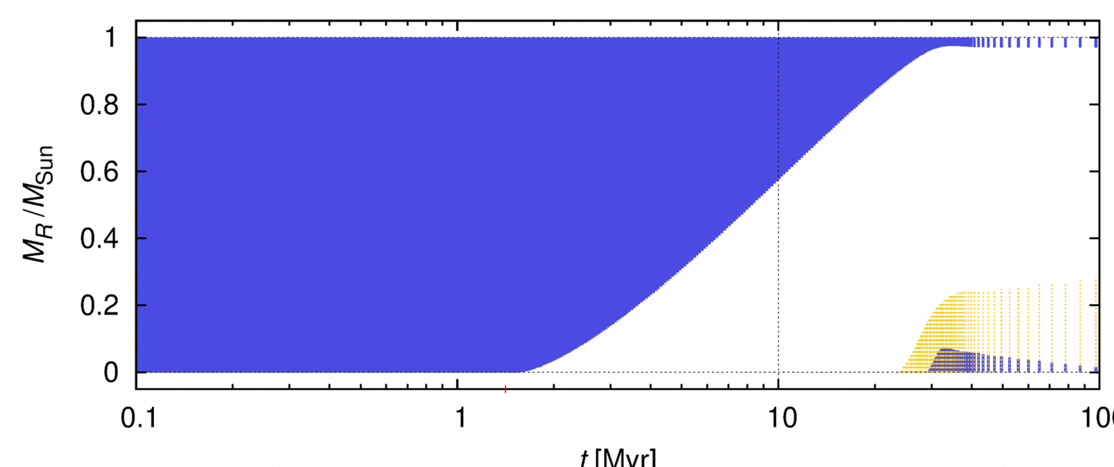

Viscosity context

ν = const. or $\nu = \alpha c_s H$

- vertical shearing instability **VSI** (a.k.a. Kelvin–Helmholtz in z direction; Nelson et al. 2013)
- subcritical baroclinic instability **SBI** (essentially, Rayleigh–Taylor with heat diffusion; Klahr & Bodenheimer 2003)
- magneto–rotational instability **MRI** (Balbus & Hawley 1973, Turner et al. 2014)
- spiral wave instability SWI (resonant coupling between spiral arms induced by an embedded planet and inertial-gravity waves; Bae et al. 2016)

$\nu = 0$

- strong stellar wind (Günther 2013, Turner et al. 2014)
- X-wind at the disk edge (Shu et al. 1994)
- magneto-centrifugal wind and loading of ions (Anderson et al. 2005, Stute et al. 2014, Bai et al. 2016)

Model ingredients (Fargo-Thorin)

- based on Fargo (Masset 2000) ← extended by OC
- N-body interactions u. Rebound (Rein & Spiegel 2015)
- inclination damping (Tanaka & Ward 2004)
- integral LTE opacities (Bell & Lin 1994)
- pebble accretion: Bondi regime, Hill r.
- Type-I migration → Type-II (gas accretion, gap opening)
- FVM discretisation $N_r = 1024$, $N_\varphi = 1563$; implicit SOR (RTE), CFL
- MPI, OpenMP
- free parameters: $\Sigma(r)$, M_{em}, $\#_{\mathrm{em}}$, $\dot{M}_{\mathrm{F}}$, ν (or α), but not $h = H/r$
- fixed parametes: $M_\odot$, $T_\odot$, $R_\odot$, α_{p}, γ, μ, c_{K}, A, Sc, ρ_{b}, f_{acc}

Case III nominal

As presented in Chrenko et al. (2017).

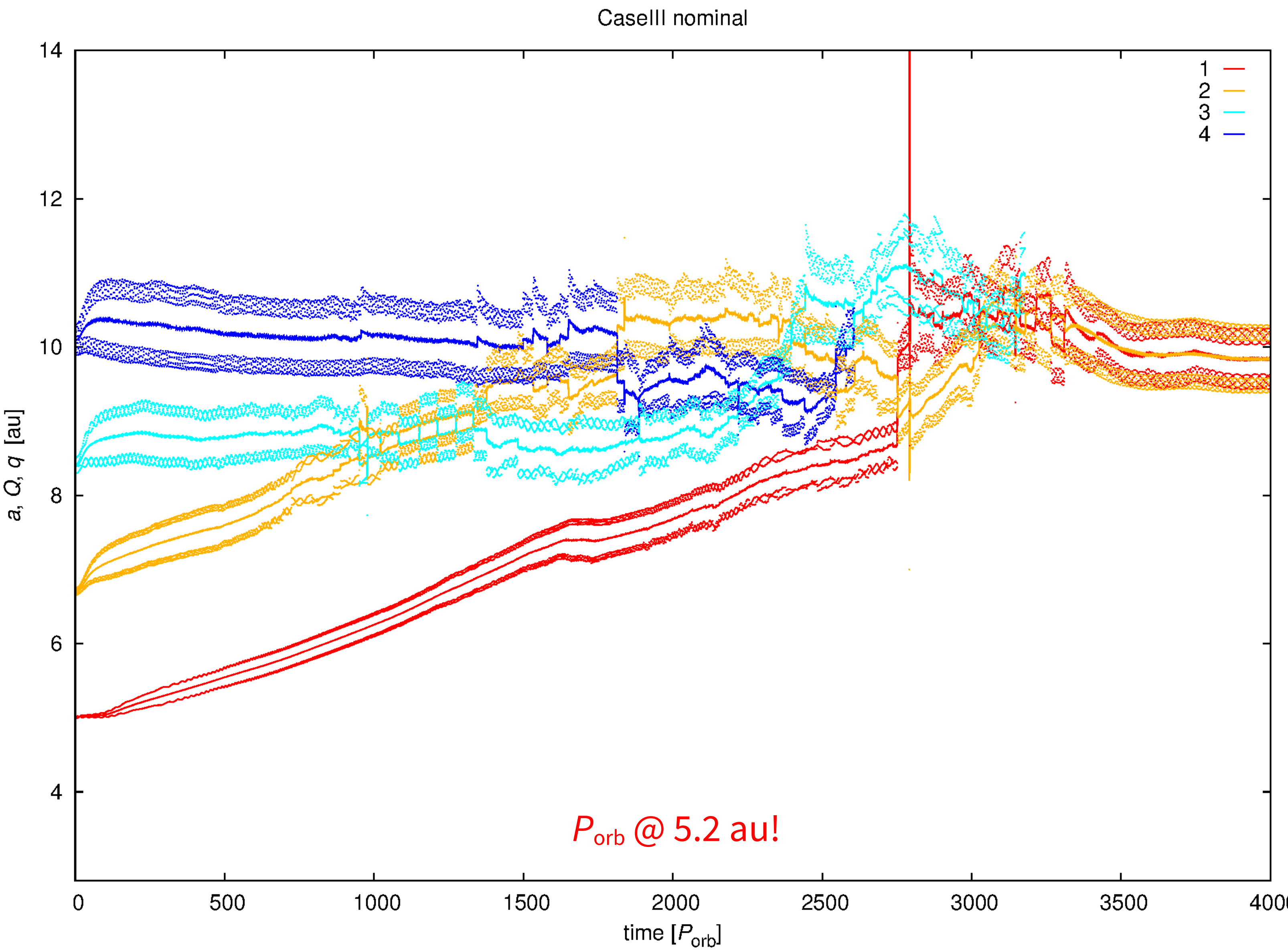

Starting with 4 embryos, 3 ME, initial spacing 10 RHill, pebble flux 2x10-4 ME per yr, approx. MMSN, with 0.5 Sigma(r) slope, kinematic viscosity nu = 1e-5 [c.u.], proto-Sun, resolution 1024x1536, damping BC's, artificial inclination damping (Tanaka & Ward 2004), no Hill cut. Results: hot-trail effect, high eccentricities (cf. talk by O. Chrenko), 0-torque at approx. 9 au, no low-order mean-motion resonances (MMR), because embryos were too close, capture difficult anyway (because e > 0), two successful mergers 13.8 ME and 4.3 ME, but co-orbitals, their long-term evolution? 3-body interactions are needed for sucessful mergers! a scattering event occurs prior to every merger (2 out of 2); see details below...

Case III nominal: Merger

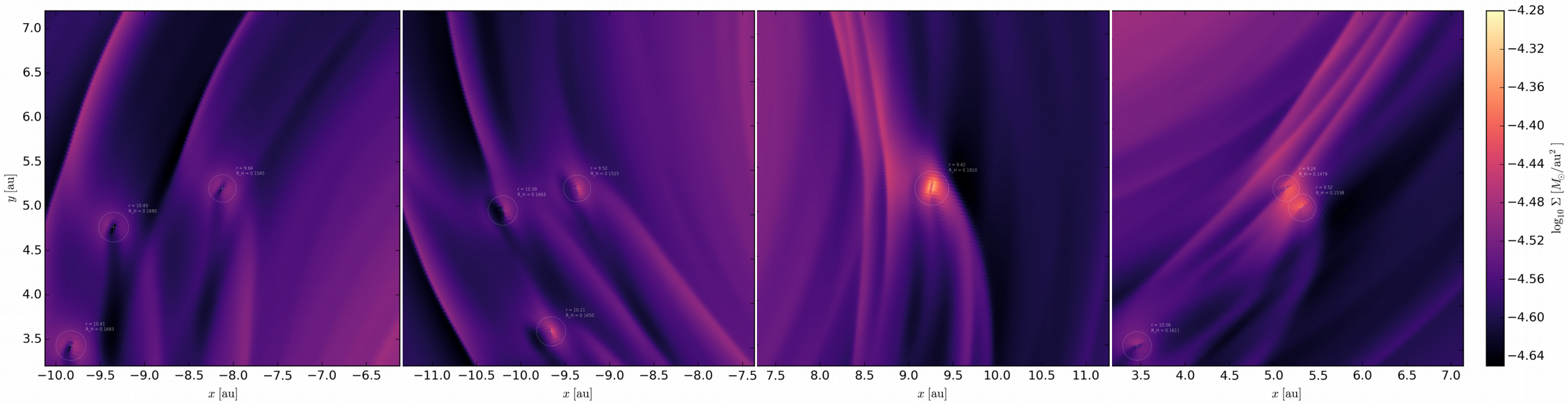

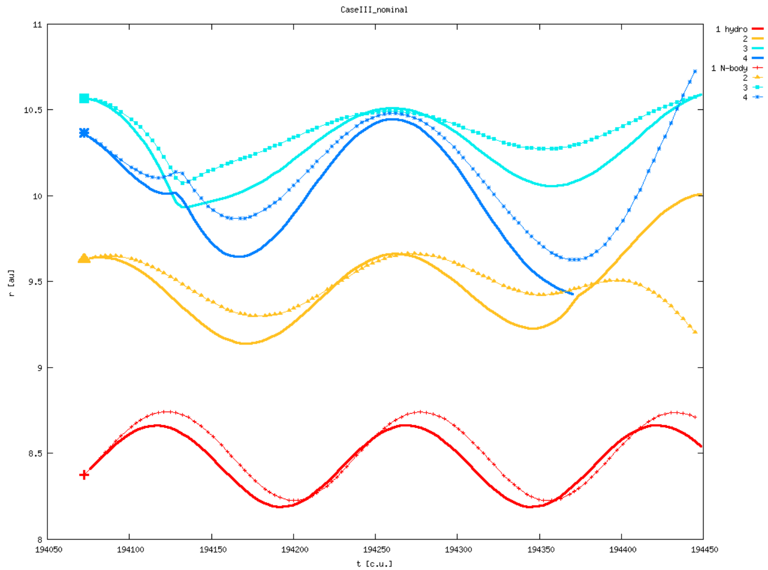

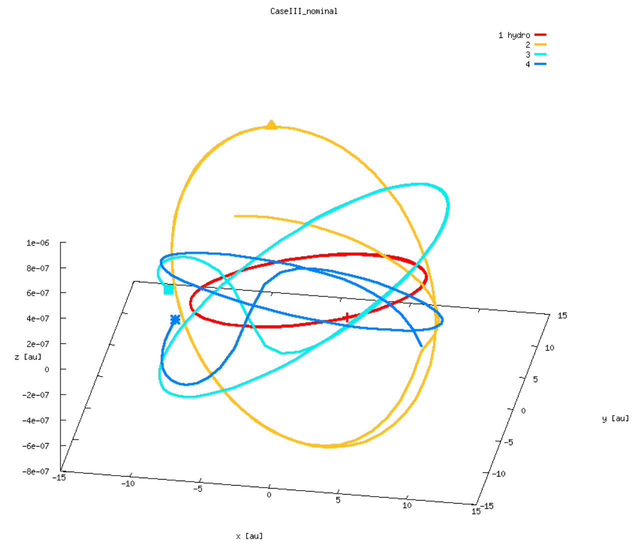

Case III nominal: Coorbital

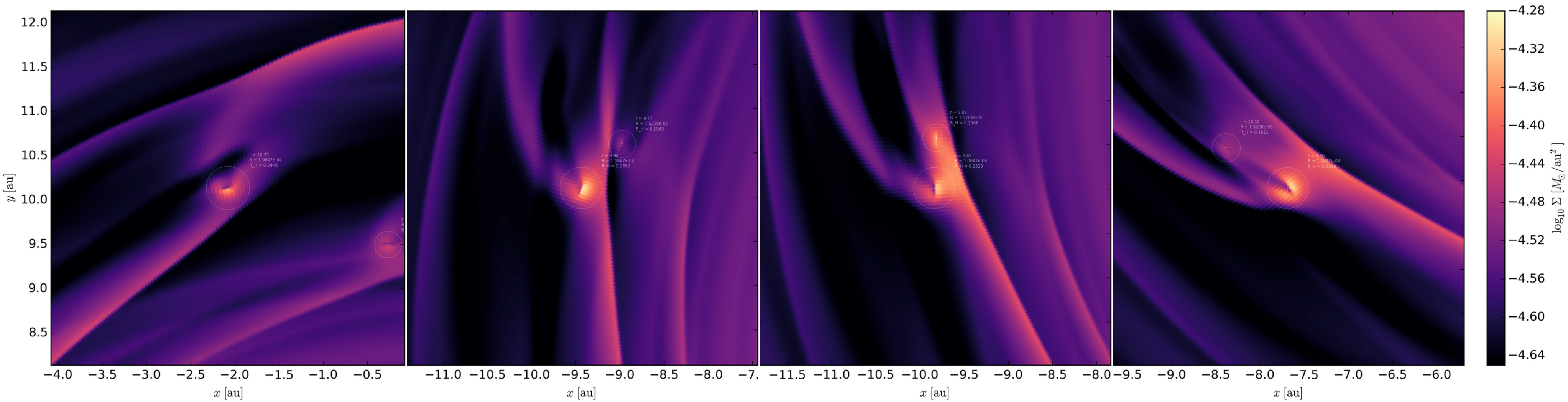

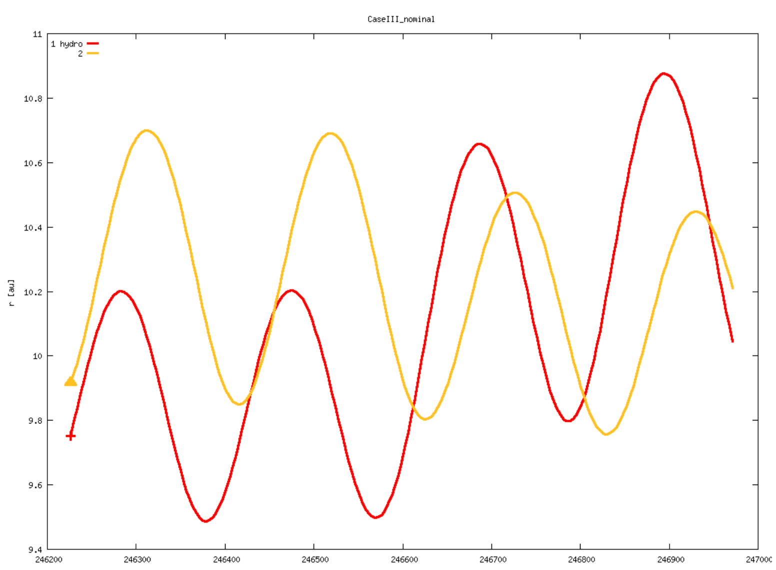

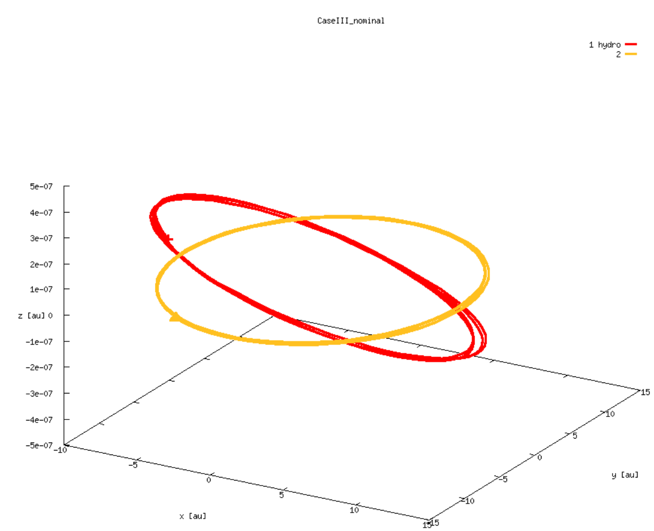

Sigma 3MMSN

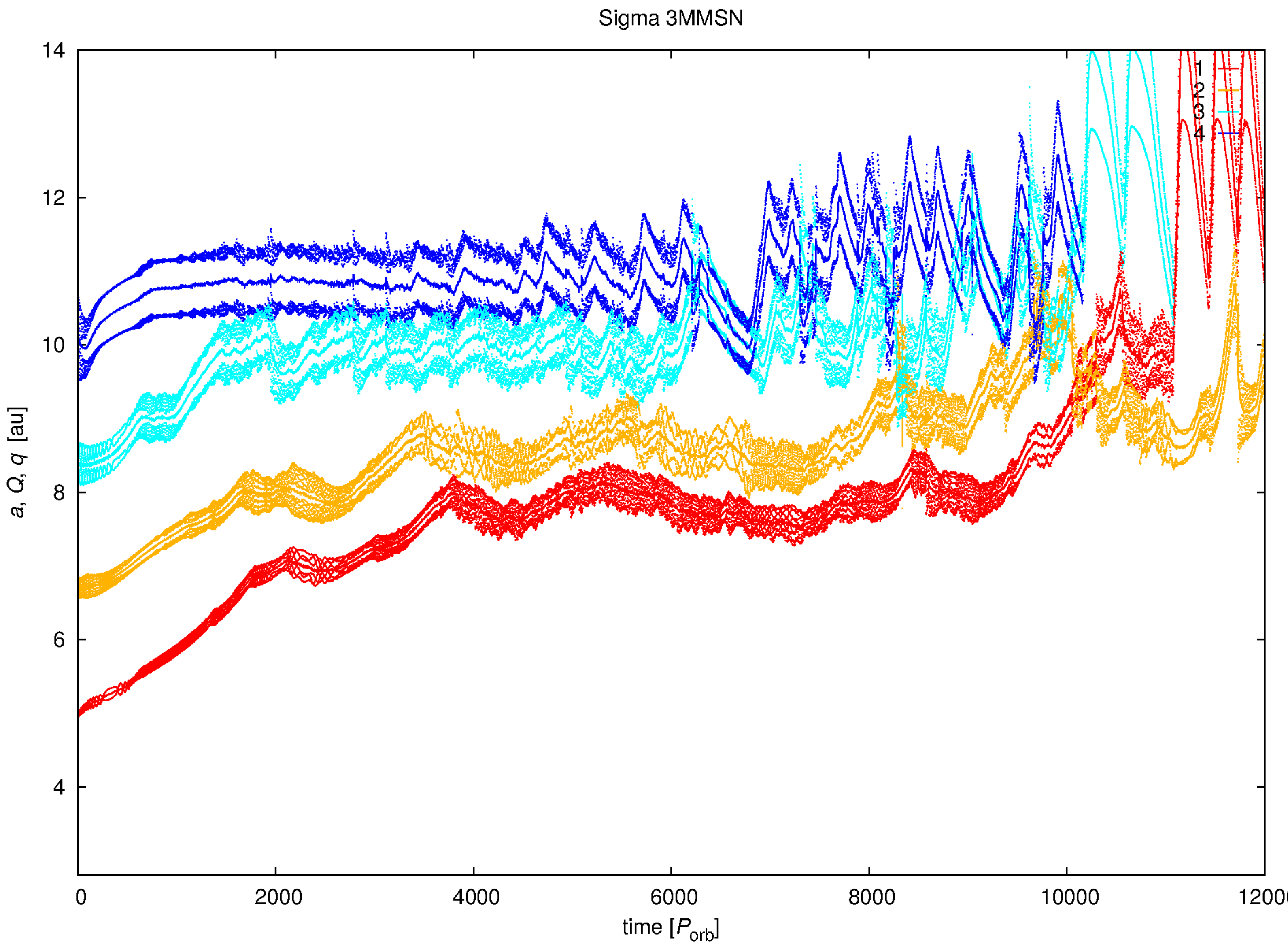

private notes: initial surface density 3x larger; 0-torque radius further out at 11 au, e often smaller, slower evolution (even though timespan 2x longer), embryos do NOT interact so strongly, rather stay next to each other, because damping is too large? sometimes inward migration of inner embryos @ larger e, possible interference of (massive) co-orbital regions? 10+ attempts of the outer 4th embryo to enter the co-orbital region of the 3rd one, only temporary coorbitals; the last part affected by interactions with the disk edge and damping zone, which kills the outer spiral arm.

Embryos 0.1M_E 120

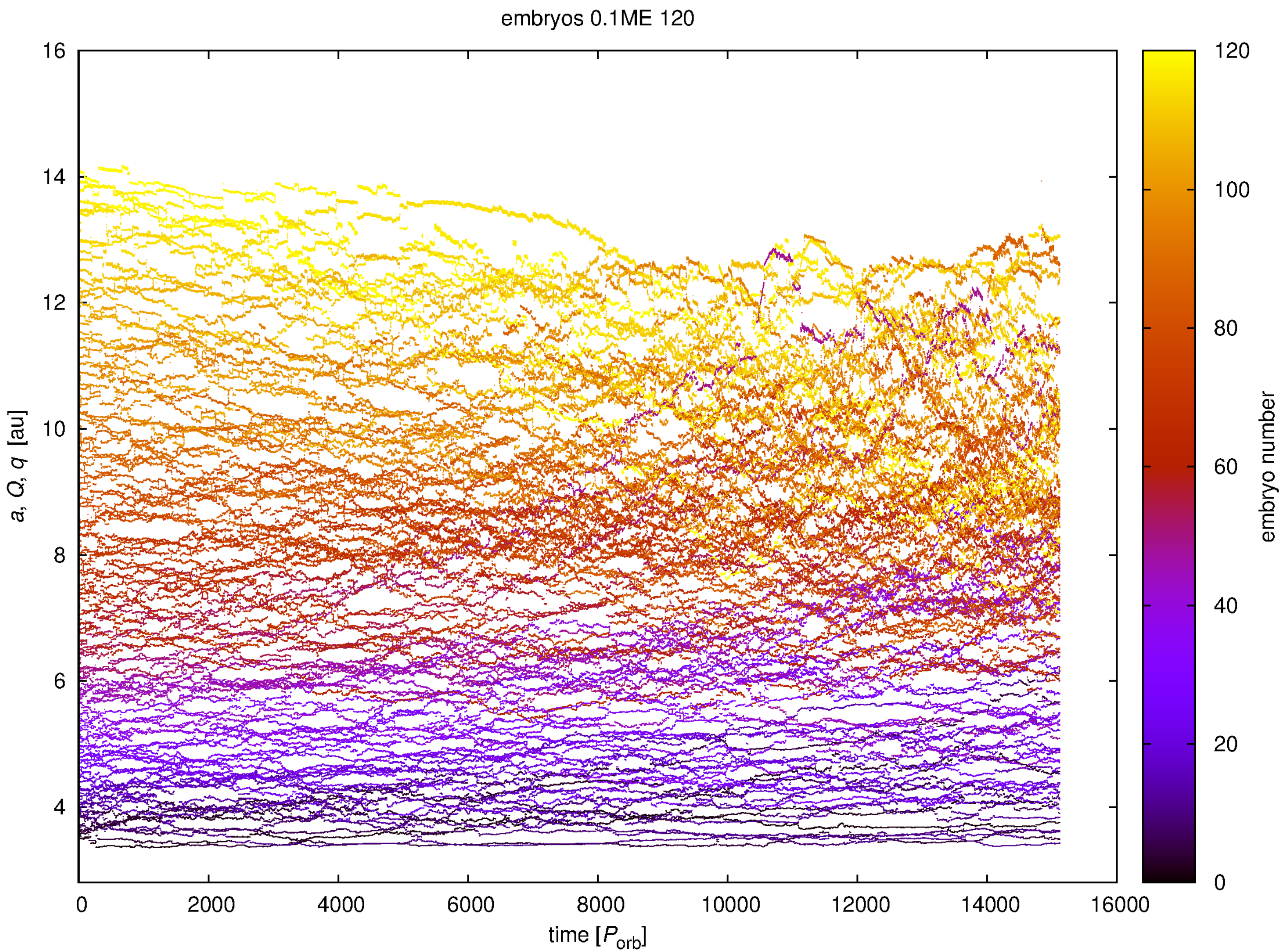

120 low-mass 0.1 ME embryos, spacing 2 mutual R Hill, disk up to 16 au, resolution still low (3 pixels per Hill sphere); overlapping weak spiral arms, slow evolution dominated by encounters, e up to 0.06, 10+ quick mergers 0.2 ME, pebble accretion up to 1.4 ME, but strong filtering for inner embryos, 0.2 ME mergers are either inside (short periods) or outside, the "winner" is outside (no filtering) - see the plot wrt. mass, or enhanced massive bodies, several mergers or pebble-accreted bodies up to 3 ME, we are apparently at the beginning of CaseIII_nominal, but the bodies concentrate in the outer disk :-|, e excitation by hot trail alone is 0.02 only, but this is NOT final value, nevertheless, it serves as an initial 'kick'!

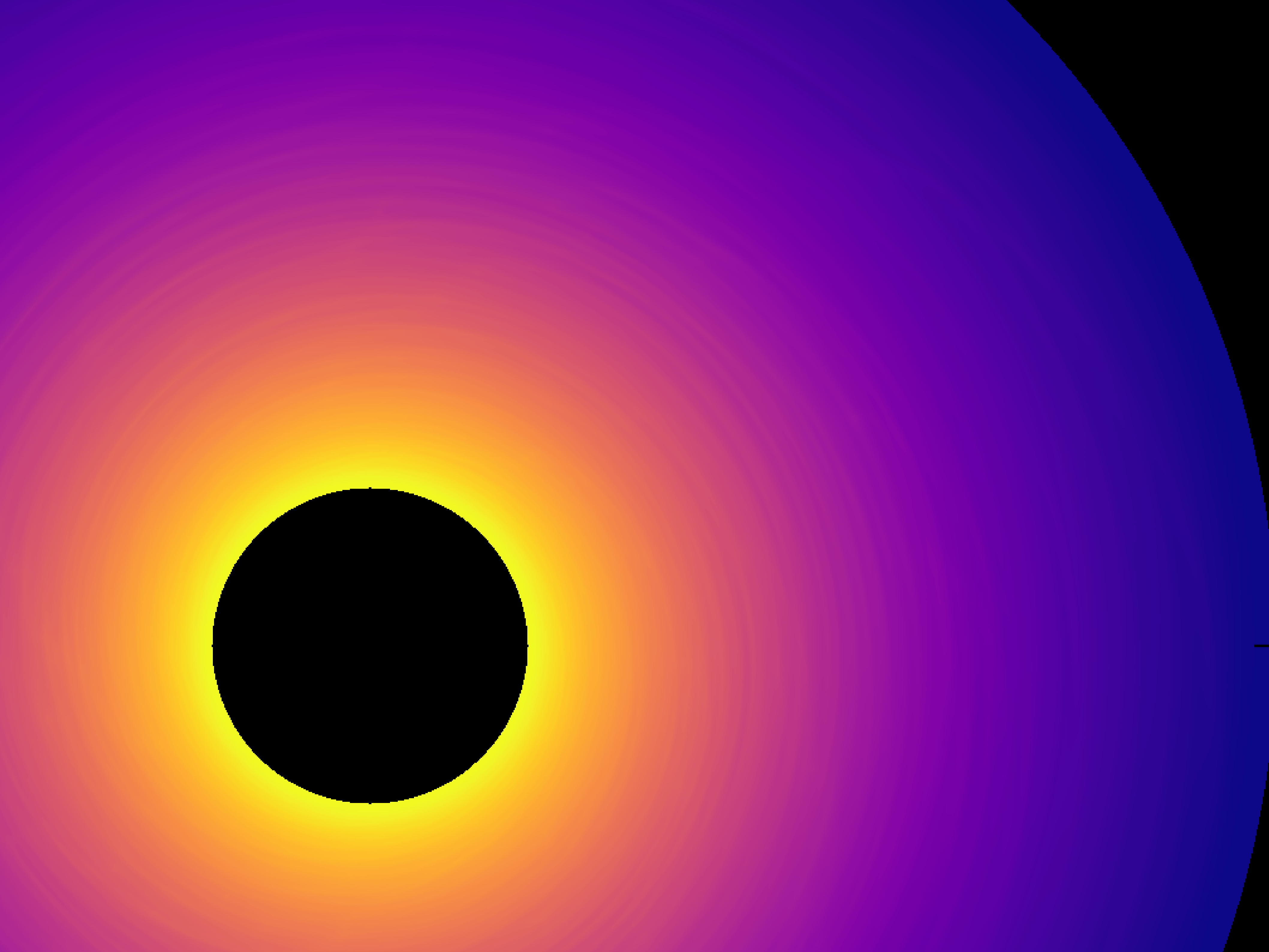

Embryos 1.5M_E 8

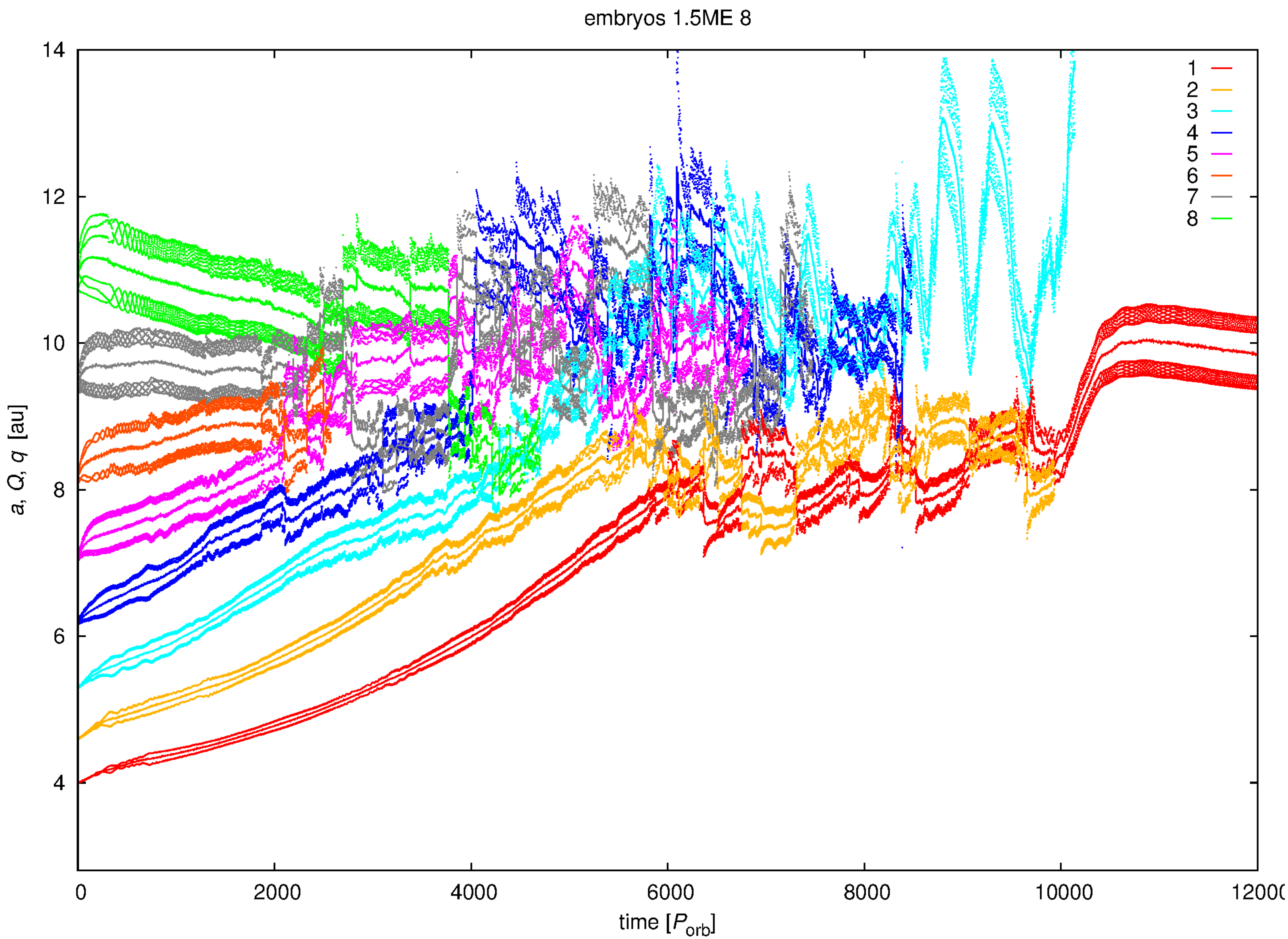

8 embryos with 1.5 M E, clear convergence to 0-torque, slower evolution, a number of encounters, more opportunities to merge, especially when an additional embryo arrives and starts to interact, several mergers, the final mass of the escaping embryo is 25 ME, the heating may be actually lower (pebble isolation), and there is NO gas accretion in this model; btw. it's strange that 5-6 ME embryos (cf. below) migrate out of the disk without problems, similar final position of the remaining embryo, more outer embryos should be added and an extended disk (20 au) should be used? is the long duration of the high pebble flux ok?

Pebbleflux 2e-5

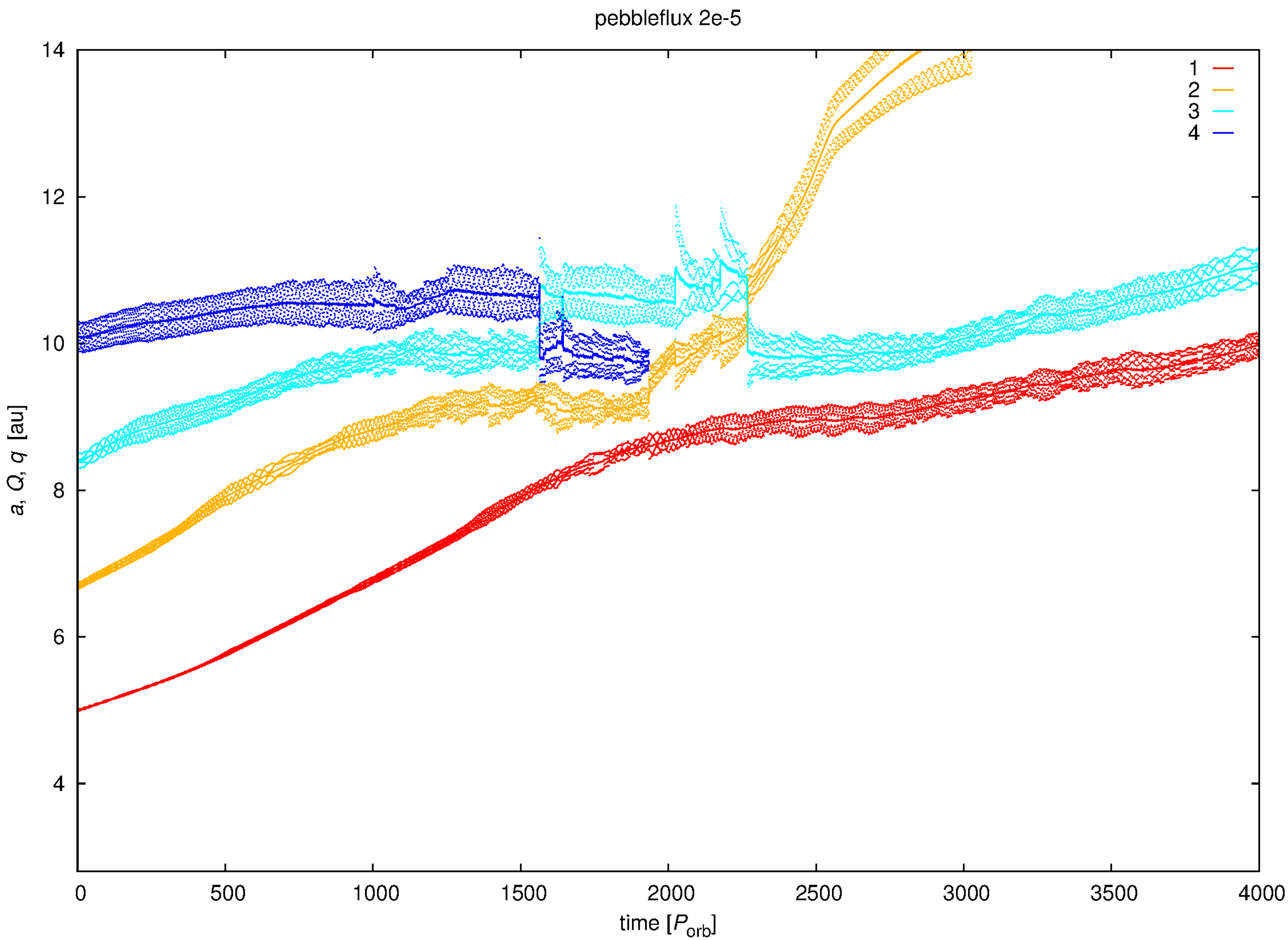

10× lower pebble flux 2×10-5 ME, i.e. 0.25 ME per 4000 Porb (more realistic?), lower eccentricity excitation (!), consequently smooth evolution, all embryos initially drift outwards, 0-torque at about 11 au? 1 yellow merger with 6 ME quickly drifts outwards (!), only temporarily decelerated by the 3rd embryo, runaway migration mode as in Pierens & Raymond (2016)? planet IX? :) Is it a rule for low pebble fluxes? Possible clearing of the outer disk? Why the 2 remaing embryos migrate outward? (initially the convergence zone is at 10 au) More outer embryos should be probably added…

Totmass 20M_E

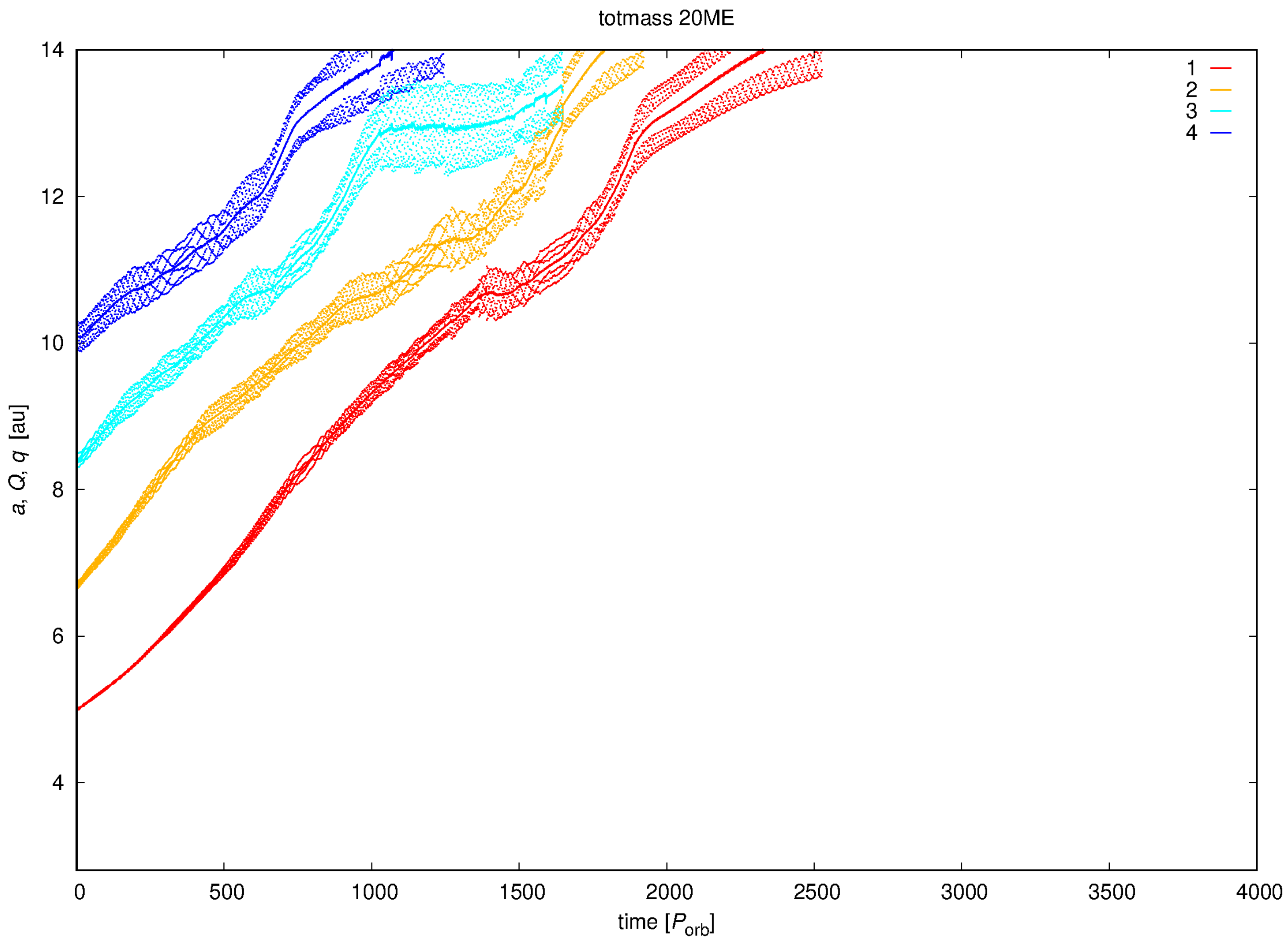

initial masses 5 M E; all embryos quickly drift outwards (!), even though wo. heating the 0-torque should be at 7 au; lower e, practically NO interactions, because real 0-torque is further out, unwanted interactions with the disk edge; larger disk & more embryos shoud be used...

Viscosity 1e-6

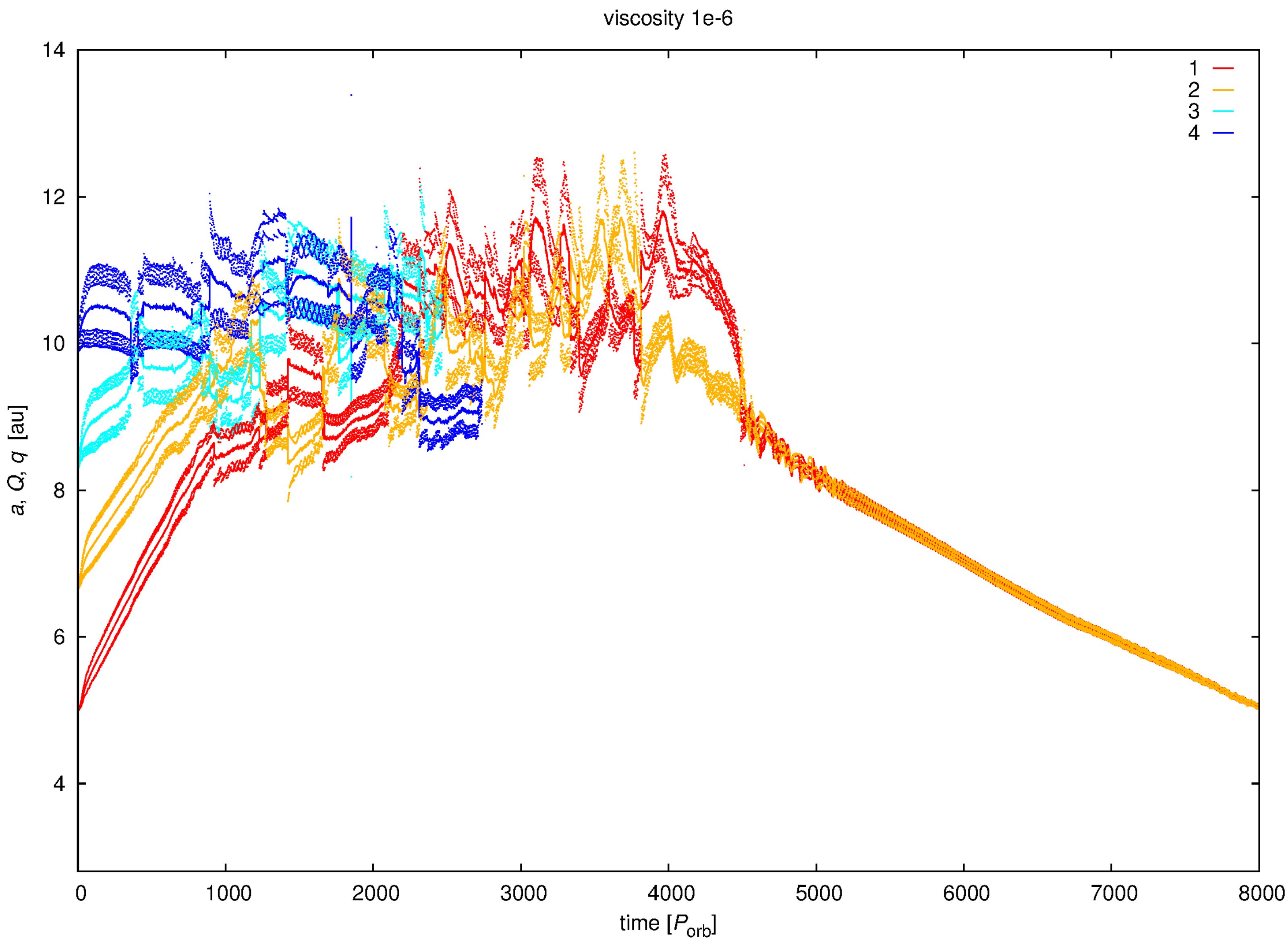

low-viscosity disk; same e, BUT faster migration da/dt, i.e. like ν in the denominator (?!), surroundings more easily affected by the embryo, many encounters, only temporary co-orbitals, 2 mergers 8 ME as of yet, an onset of gap opening even without gas-accretion term? many attempts to form a co-orbital pair, finally a coorbital is formed and further stabilised, a change of regime around t = 4500 P_orb is due to developed pebble isolation (see below)

Viscosity 1e-6: Exchange

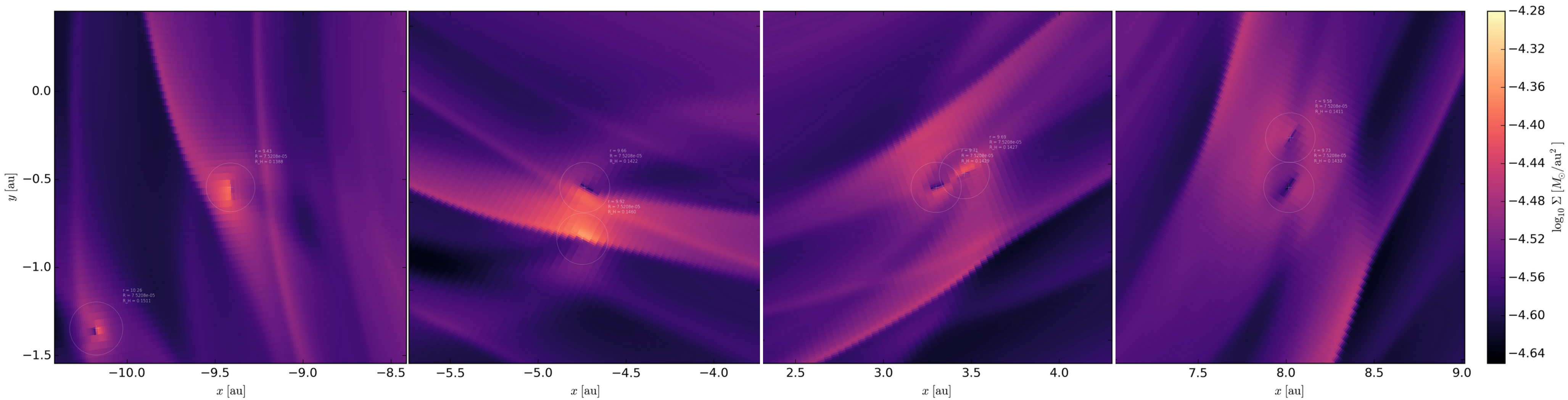

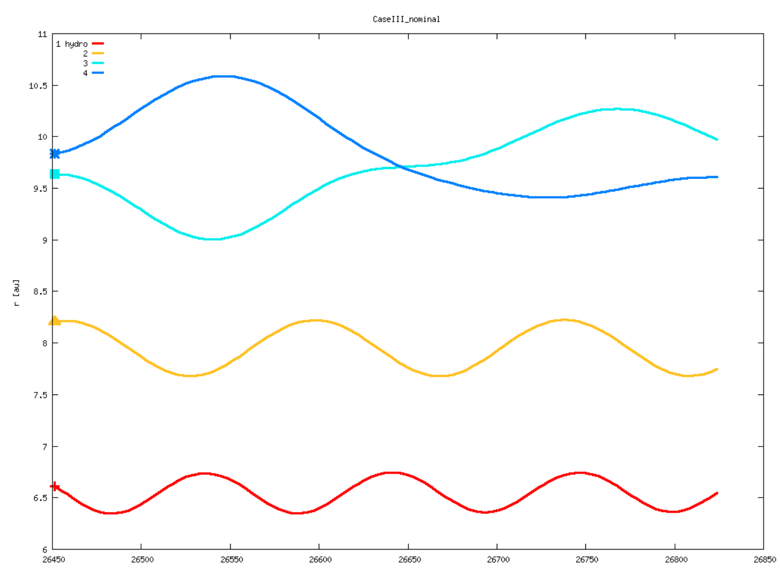

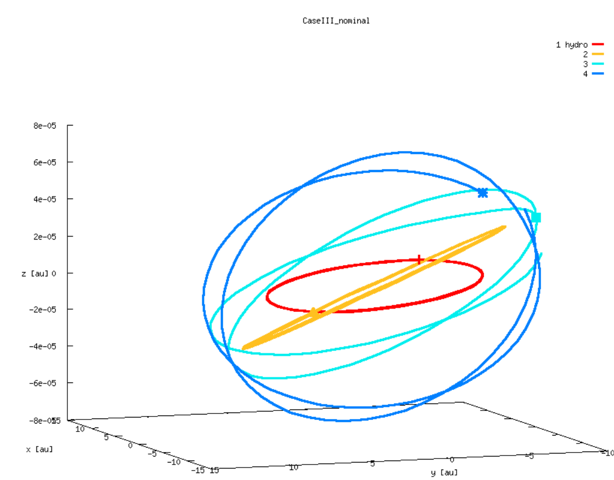

The Bet :: Sigma 1over3

Q: Will the hot trail effect be smaller or larger for $\Sigma = \frac{1}{3}\Sigma_{MMSN}$?

$\Sigma \rightarrow 0$: no gas, no perturbation, $e = 0$

$\Sigma \rightarrow \infty$: large thermal capacity, no ΔT, no expansion, $e = 0$

Sigma 1over3

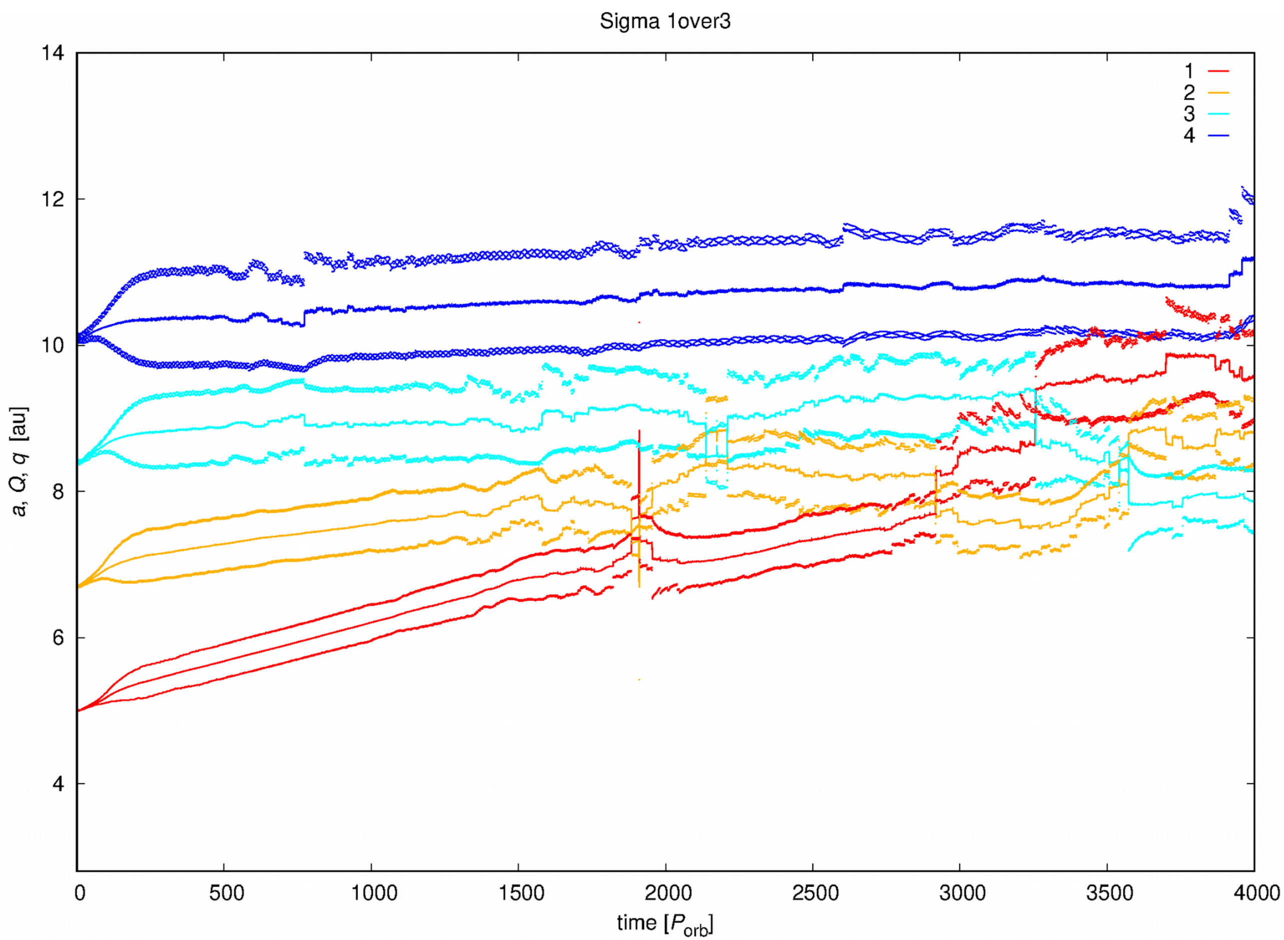

A: The hot-trail effect is *larger* (and seems more stable)!

Conclusion: Evolution does depend on parameters! (surprisingly)

↑ migration map difficult

Hidden problems

- **2D → 3D**
- hot trail in *l*, pebble isolation (Eklund & Masset 2017, Bitsch etal. 2018)
- LTE, no * ← falling snowflakes
- mean-field, no outliers
- inner edge setup (stability)
- unresolved turbulence ← ν *isn't* free
- resolution for small masses! ← discretisation errors, N^4 scaling
- opacity in FUV, V? ← sideways irradiation, windows
- inflow vs outflow, advective atmospheres (Lambrechts & Lega 2017)
- GPUs (Benítez-Llambay & Masset 2016)

Q: How to resolve disks (IC)?

- photometry (unresolved)
- interferometry, spectro-interferometry, w. supersythesis
- absolute SED, calibrated flux F_λ [erg s cm^{-2} cm^{-1}]
- differential interferometry (in line profiles)
- spectroscopy, a.k.a. Doppler tomography

- IFT difficult, if not impossible ← audio vs video, distorted image
- synthetic image && DFT

Model (Pyshellspec)

← based on Shellspec (Budaj 2011)

+ LTE level populations
+ LTE ionisation levels
+ 1D line-of-sight transfer
− optically-thin (single) scattering ← no 3D, LI or ALI!
− non-isotropic scattering
+ prescribed ρ, T profiles
+ solar abundances
+ Voigt profile (prior to D.)
+ thermal broadening
+ microturbulence
+ natural
+ Stark
+ Van der Waals
+ Doppler shift
+ HI bound-free continuum opacity
+ HI free-free
+ H free-free

− Thomson scattering on free electrons
− Rayleigh scattering on neutral hydrogen
− Mie absorption on dust
− Mie scattering
− dust thermal emission
− line opacity
+ spherical primary (gainer)
+ Roche secondary (donor)
− black-body approximation (for *)
+ synthetic spectra (for *)
− irradiation
− reflection
+ limb darkening
+ gravity darkening
− heat transport

$$I_\nu(0) = \int_0^{\tau_\nu} S_\nu \, \mathrm{e}^{-\tau'_\nu} \, \mathrm{d}\tau'_\nu + I^\star_\nu(\nu_2) f_{\mathrm{LD}} \, \mathrm{e}^{-\tau_\nu}$$

$$S_\nu = \frac{\epsilon_\nu}{\chi_\nu}$$

$$\nu_2 = \nu \left(1 - \frac{v^\star_z}{c}\right)$$

$$\chi_\nu = \kappa_\nu + \sigma_\nu$$

$$\kappa_\nu = \kappa_\nu^{\mathrm{line}} + \kappa_\nu^{\mathrm{odf}} + \kappa_\nu^{\mathrm{HIbf}} + \kappa_\nu^{\mathrm{HIff}} + \kappa_\nu^{\mathrm{H^-bf}} + \kappa_\nu^{\mathrm{H^-ff}}$$

$$\sigma_\nu = \sigma_\nu^{\mathrm{TS}} + \sigma_\nu^{\mathrm{RS}}$$

$$\epsilon_\nu = \epsilon_\nu^{\mathrm{th}} + \epsilon_\nu^{\mathrm{sc}}$$

$$\epsilon_\nu^{\mathrm{th}} = B_\nu(T(z))\kappa_\nu$$

$$\epsilon_\nu^{\mathrm{sc}} \doteq \sigma_\nu I^\star_\nu f_{\mathrm{SH}} \frac{\omega}{4\pi}$$

Young experiment

- monochromatic vs polychromatic vs extended
- experiment: waves and shadows

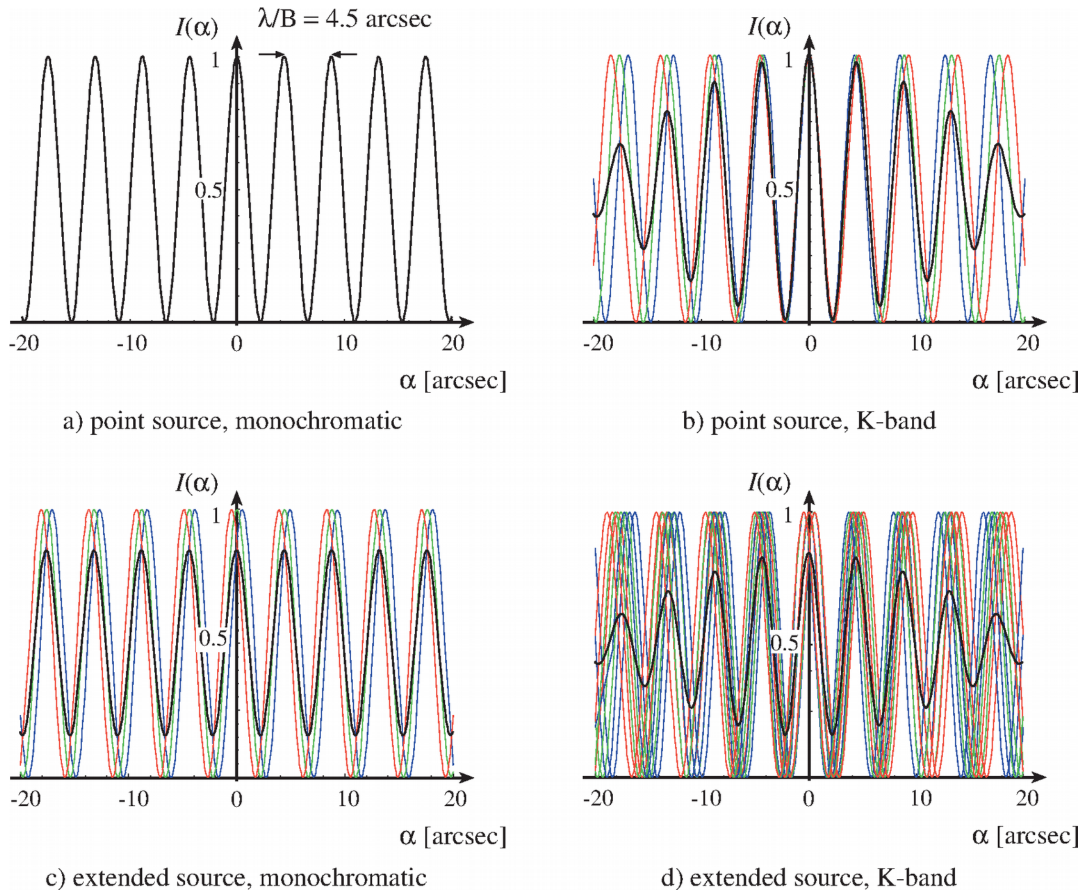

Glindeman (2008)
AFY

Young experiment (cont.)

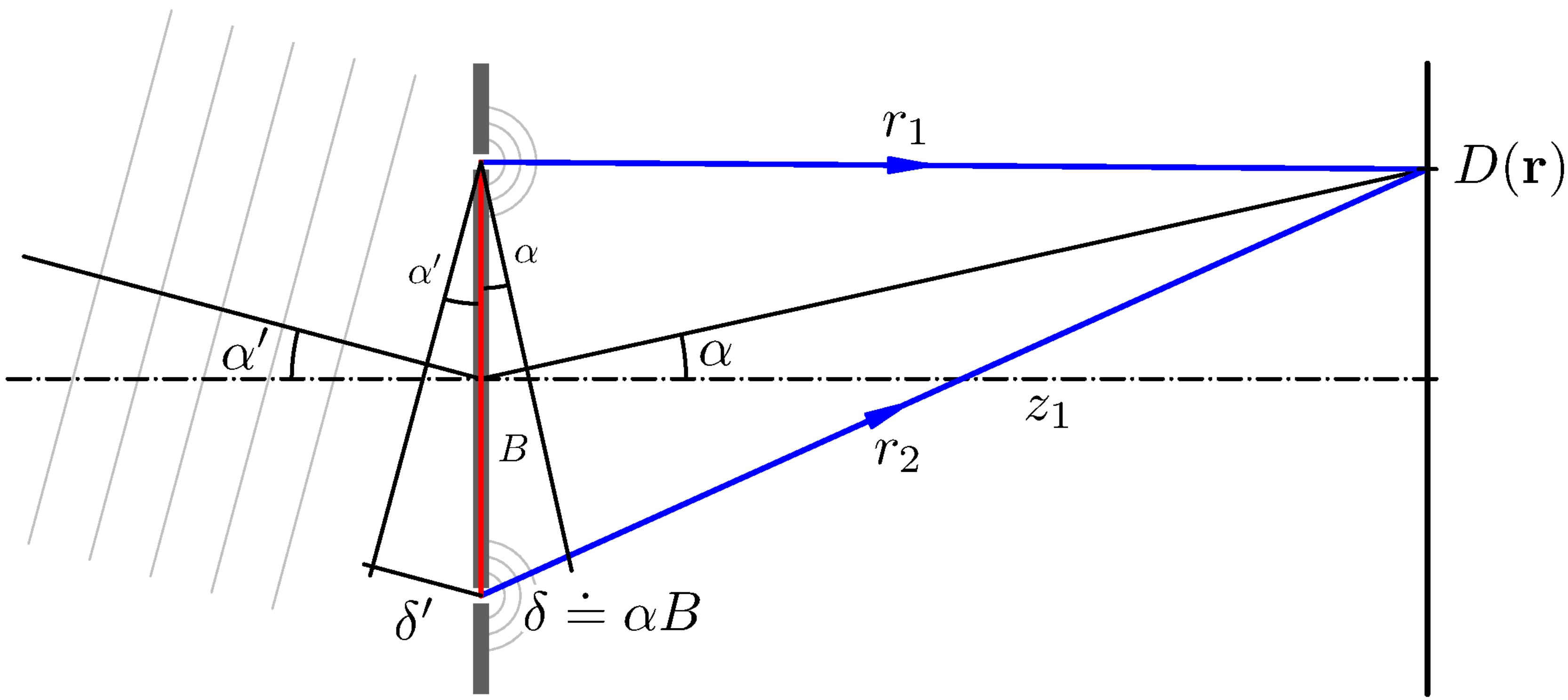

Obrázek 6.51: Uspořádání Youngova experimentu, kde B označuje vzájemnou vzdálenost štěrbin (základnu), z_1 vzdálenost stínítka od překážky, r_1, r_2 vzdálenost studovaného místa na stínítku od štěrbin, α odpovídající odchylka od osy překážky, α' úhel dopadu vlny na překážku, δ, δ' dráhové rozdíly vznikající za a před překážkou.

Visibility

Brož & Wolf (2017)

Viditelnost. V Youngově experimentu dopadá na zmiňovanou překážku rovinná monochromatická elektromagnetická vlna. Namísto jednotlivých složek polí $\mathbf{E}$, $\mathbf{B}$ budeme používat bezrozměrný vzruch D (angl. disturbance) v komplexní notaci:

$$D(\mathbf{r}, t) = D_0\, \mathrm{e}^{-\mathrm{i}(\omega t - \mathbf{k}\cdot\mathbf{r})} = D(\mathbf{r})\, \mathrm{e}^{-\mathrm{i}\omega t}\,, \tag{6.151}$$

kde $\omega = \frac{2\pi c}{\lambda}$ označuje úhlovou frekvenci a $\mathbf{k}$ vlnový vektor, $k = \frac{2\pi}{\lambda}$. Podle Huygensova principu spočteme vzruch na stínítku jako součet dvou kulových vln, šířících se z otvorů (obr. 6.51):

$$\begin{aligned} D(\mathbf{r}) &= \frac{D_0}{r_1}\, \mathrm{e}^{\mathrm{i}kr_1} + \frac{D_0}{r_2}\, \mathrm{e}^{\mathrm{i}kr_2} \doteq \frac{D_0}{z_1} \left(\mathrm{e}^{\mathrm{i}kr_1} + \mathrm{e}^{\mathrm{i}kr_2}\right) = \\ &= \frac{D_0}{z_1}\, \mathrm{e}^{\mathrm{i}\frac{1}{2}k(r_1+r_2)}\, 2\cos[\tfrac{1}{2}k(r_1 - r_2)]\,. \end{aligned} \tag{6.152}$$

Nepozorujeme ovšem přímo D, nýbrž tok daný Poyntingovým vektorem $\mathbf{S} = \mathbf{E}\times\mathbf{H}$, který lze pro naše účely středovat, normalizovat a považovat za bezrozměrnou intenzitu:

$$I(\mathbf{r}) \equiv \langle DD^* \rangle = |D(\mathbf{r})|^2\,. \tag{6.154}$$

Visibility (cont.)

V místě odchýleném od osy překážky o úhel α je pak:

$$
\begin{aligned}
I(\alpha) &= |D(\alpha)|^2 = \left(\frac{D_0}{z_1}\right)^2 4\cos^2[\tfrac{1}{2}k(r_1 - r_2)]\} = \left(\frac{D_0}{z_1}\right)^2 2\{1 + \cos[k(r_1 - r_2)]\} = \\
&\doteq I_0\{1 + \cos[k\alpha B]\}\,, \qquad (6.155)
\end{aligned}
$$

kde B označuje vzájemnou vzdálenost otvorů. Pokud navíc vlna sama dopadá na překážku pod úhlem α':

$$I(\alpha, \alpha') = I_0\{1 + \cos[k(\alpha + \alpha')B]\}\,. \qquad (6.156)$$

Jako jednoslovný popis jevu se zavádí *viditelnost*, neboli kontrast interferenčních proužků:

$$\mathcal{V} \equiv \frac{I_{\max} - I_{\min}}{I_{\max} + I_{\min}}\,. \qquad (6.157)$$

Protože zde $I_{\min} = 0$, $I_{\max} = 1$, je $\mathcal{V} = 1$. Pro rozlehlý zdroj nebo polychromatické záření bývá ovšem viditelnost menší, protože přicházející vlny nejsou prostorově respektive časově koherentní (viz obr. 6.52).

Van Cittert & Zernike theorem

Teorém van Citterta a Zernikeho. Budeme-li přes rozlehlý zdroj (úhly α') integrovat:

$$I(\alpha) = \int I(\alpha, \alpha')\mathrm{d}\alpha' = \overbrace{\int I(\alpha')\mathrm{d}\alpha'}^{= I_0} + \overbrace{\int I(\alpha')\cos[k(\alpha+\alpha')B]\mathrm{d}\alpha'}^{= \Re[\mathrm{e}^{\mathrm{i}k\alpha B}\int I(\alpha')\,\mathrm{e}^{\mathrm{i}k\alpha' B}\,\mathrm{d}\alpha']}\,, \qquad (6.158)$$

uzříme, že se vlastně jedná o reálnou část Fourierovy transformace rozložení intenzity zdroje $I(\alpha')$, násobené jakýmsi faktorem. Obecněji zapsáno:

$$I(\vec{\alpha}) = I_0 \left\{1 + \Re\left[\mu(\vec{B})\,\mathrm{e}^{-\mathrm{i}k\vec{\alpha}\cdot\vec{B}}\right]\right\}\,, \qquad (6.159)$$

kde komplexní *funkce viditelnosti*:

$$\mu(\vec{B}) \equiv \frac{\int I(\vec{\alpha}')\,\mathrm{e}^{-\mathrm{i}k\vec{\alpha}'\cdot\vec{B}}\,\mathrm{d}\alpha'}{I_0}\,, \qquad (6.160)$$

tj. tvrzení teorému van Citterta a Zernikeho. Absolutní hodnota $|\mu(\vec{B})|$ evidentně určuje viditelnost $\mathcal{V}$ (tj. kontrast), kdežto příslušná fáze $\phi(\vec{B})$ polohu „prostředního“ bílého proužku.

Closure phase ← asymmetry of the source!

Vzruch je na každém z dalekohledů pozměněn (Haniff 2006):

$$\tilde{D} = GD = |G|\,\mathrm{e}^{\mathrm{i}\Phi} D\,, \tag{6.169}$$

kde $|G|$ označuje zisk dalekohledu, zohledňující mj. odrazivost zrcadla, Φ fázový posun, ovlivněný seeingem, teplotní roztažností atd. Funkce viditelnosti je přitom $\mu \propto D_1 D_2^*$, čili skutečně měřená („rozvlněná“) funkce viditelnosti:

$$\tilde{\mu} = G_1 G_2^*\,\mu = |G_1||G_2|\,\mathrm{e}^{\mathrm{i}(\Phi_1-\Phi_2)}\mu\,. \tag{6.170}$$

Amplituda je evidentně zmenšena, fáze kamsi posunuta. Definujeme-li však *trojný součin* (zvaný též bispektrum):

$$T_3 \equiv \mu_{12}\mu_{23}\mu_{31}\,, \tag{6.171}$$

zjistíme úžasnou věc:

$$\begin{aligned} \tilde{T}_3 &= \tilde{\mu}_{12}\tilde{\mu}_{23}\tilde{\mu}_{31} = \\ &= |G_1||G_2|\,\mathrm{e}^{\mathrm{i}(\Phi_1-\Phi_2)}\mu_{12}\,|G_2||G_3|\,\mathrm{e}^{\mathrm{i}(\Phi_2-\Phi_3)}\mu_{23}\,|G_3||G_1|\,\mathrm{e}^{\mathrm{i}(\Phi_3-\Phi_1)}\mu_{31} = \\ &= |G_1|^2|G_2|^2|G_3|^2\mu_{12}\mu_{23}\mu_{31}\,. \end{aligned} \tag{6.172}$$

Amplituda je sice zmenšena, ale fáze nikam *neposunuta*! Uzavírací fáze je pak $\arg T_3$.

Fringes (for VLTI)

- D = 8 m, B = 100 m, observations of a disk θ = 1 or 5 mas,

  but without seeing, bandwidth $\Delta\lambda_{\mathrm{eff}}$, and other incoherence

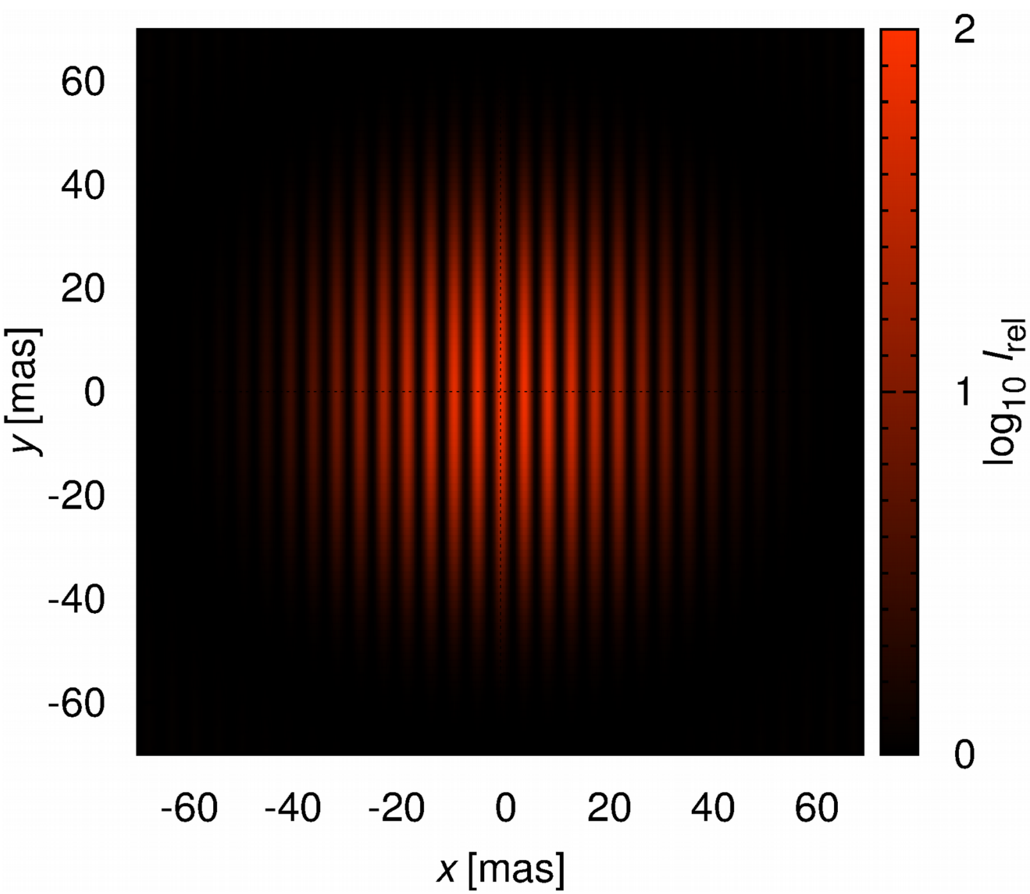

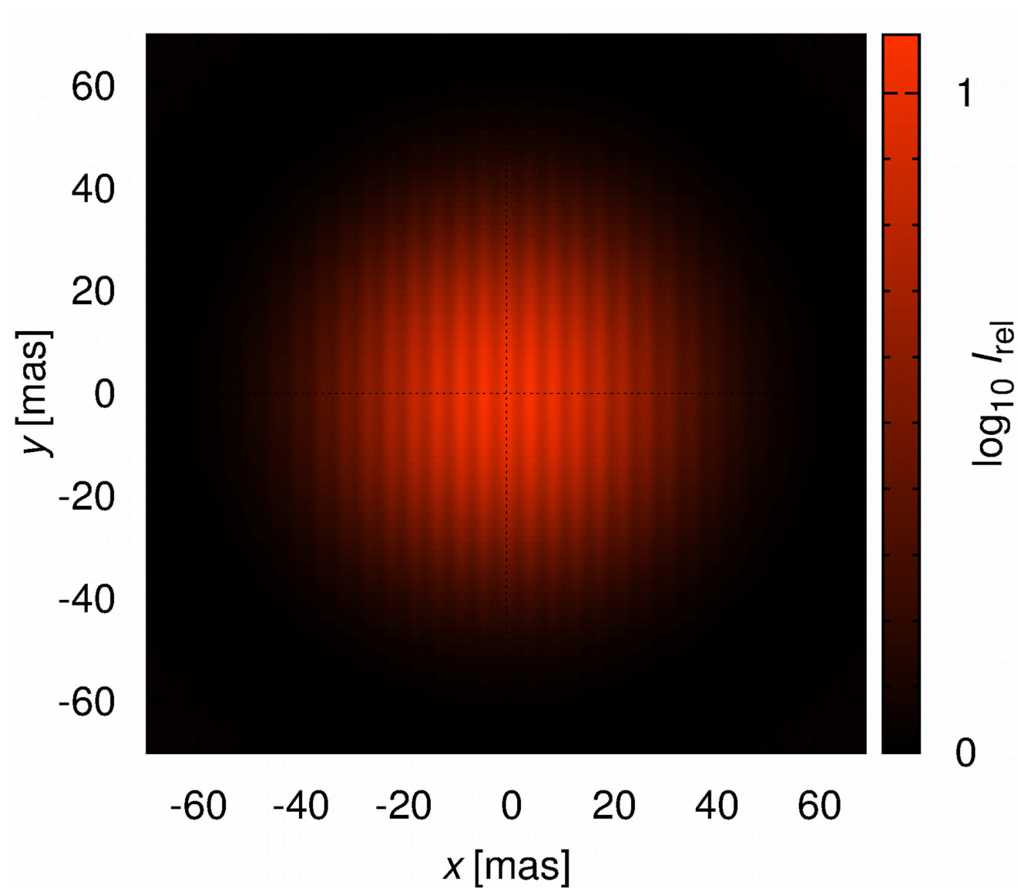

CHARA

- Mt. Wilson observatory, 6 telescopes, Y configuration, 10 baselines up to 331 m, B/λ = 331 m/550 nm = $6 \cdot 10^8$ c. per b.
- Mersenne afocal system, primary diameter 1 m (ten Brummelaar et al. 2005)

Optical scheme

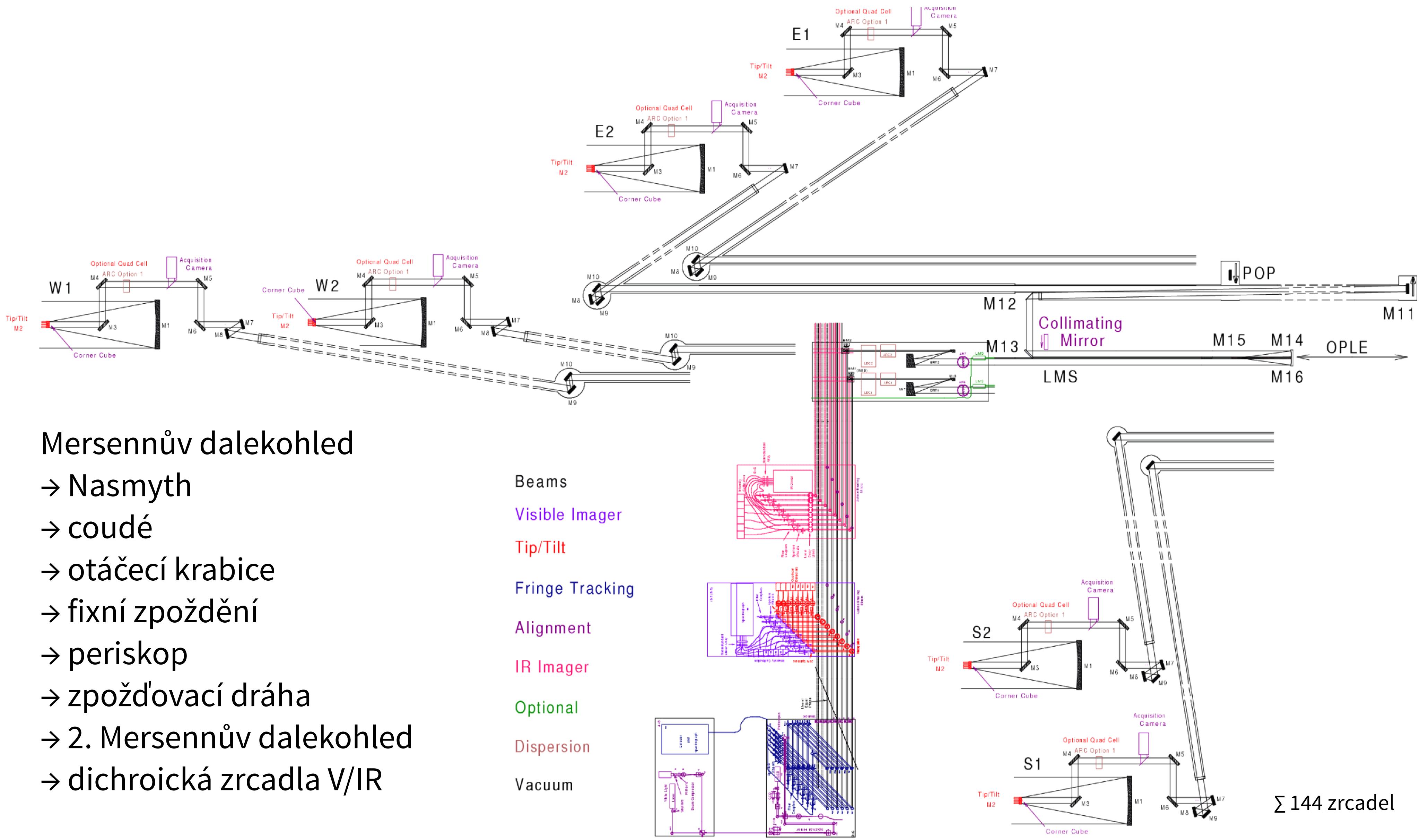

Mersennův dalekohled
→ Nasmyth
→ coudé
→ otáčecí krabice
→ fixní zpoždění
→ periskop
→ zpožďovací dráha
→ 2. Mersennův dalekohled
→ dichroická zrcadla V/IR

∑ 144 zrcadel


OPLE
Periscopes
PoPs
Metrology
BRT
LDC
BSS
EXIT

Model (cont.)

- Python interface by JN — http://sirrah.troja.mff.cuni.cz/~mira/betalyr/
- computation of interferometric observables (DFT), joint χ^2
- multiprocessing module (split on wavelengths; 4-8 cores)
- discretisation $N_x = 160$, $N_y = 60$ (~1 $R_\odot$); variable in z (~τ)

  ↑ trapezoidal rule
- local & global optimisation (DE, simplex, ...)
- 1 iteration: 2392 synthetic images per iteration (3 min),
  1 convergence: $>10^3$ steps (several days)
- free parameters: H (or θ), $R_{\rm out}$, ρ, T_0 (or T_1), $\alpha_{\rm D}$, $\alpha_{\rm T}$, i, Ω, d, $h_{\rm inv}$, $t_{\rm inv}$, $h_{\rm wind}$, $h_{\rm mul}$
- fixed parameters: P, JD$_{\rm min}$, $\dot{P}$, $a \sin i$, M_1, $q = M_1/M_2$, e, ω, $f_{\rm ill}$, $R_{\rm g}$, $T_{\rm eff,d}$, $T_{\rm eff,g}$, $x_{\rm bol,d}$, $x_{\rm bol,g}$, $\alpha_{\rm gd,d}$, $\alpha_{\rm gd,g}$, ...

Joint χ^2 metric

$$\chi^2_{\mathrm{LC}} = \sum_{i=1}^{N_{\mathrm{P}}} \sum_{j=1}^{N_{\mathrm{M}}} \left(\frac{m^{\mathrm{obs}}_{i,j} - \tilde{m}^{\mathrm{syn}}_{i,j}}{\sigma_{i,j}} \right)^2 ,$$

$$\chi^2_{\mathrm{IF}} = \chi^2_{\mathrm{IF_{VEGA}}} + \chi^2_{\mathrm{IF_{NPOI}}} + \chi^2_{\mathrm{IF_{MIRC}}} ,$$

$$\chi^2_{\mathrm{IF_{VEGA}}} = \chi^2_{\mathrm{V^2}} ,$$

$$\chi^2_{\mathrm{IF_{NPOI}}} = \chi^2_{\mathrm{V^2}} + \chi^2_{\mathrm{CP}} ,$$

$$\chi^2_{\mathrm{IF_{MIRC}}} = \frac{1}{2}\left(\chi^2_{\mathrm{V^2}} + \chi^2_{\mathrm{T_3}}\right) + \chi^2_{\mathrm{CP}} ,$$

$$\chi^2_{\mathrm{V^2}} = \sum_{i=1}^{N_{\mathrm{V2}}} \left(\frac{\left|V^{\mathrm{obs}}\right|^2_i - \left|V^{\mathrm{syn}}\right|^2_i}{\sigma_i} \right)^2 ,$$

$$\chi^2_{\mathrm{T_3}} = \sum_{i=1}^{N_{\mathrm{T_3}}} \left(\frac{\left|T_3^{\mathrm{obs}}\right|_i - \left|T_3^{\mathrm{syn}}\right|_i}{\sigma_i} \right)^2 ,$$

$$\chi^2_{\mathrm{CP}} = \sum_{i=1}^{N_{\mathrm{T_3}}} \left(\frac{T_3\phi^{\mathrm{obs}}_i - T_3\phi^{\mathrm{syn}}_i}{\sigma_i} \right)^2 .$$

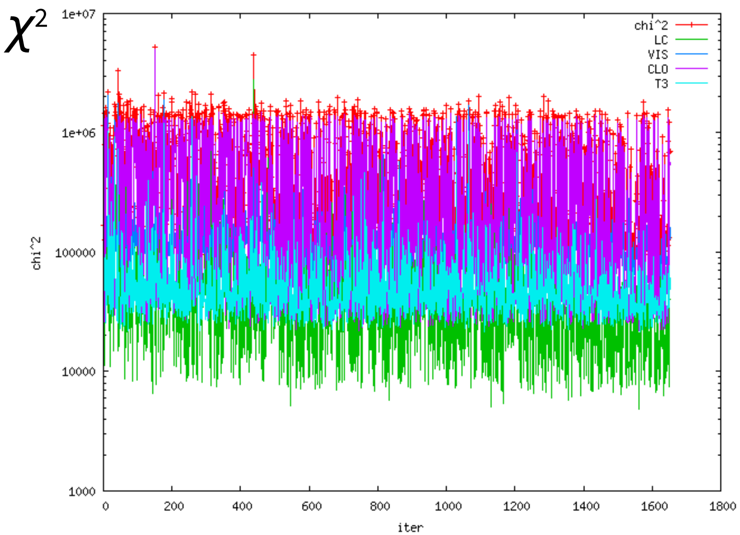

DE

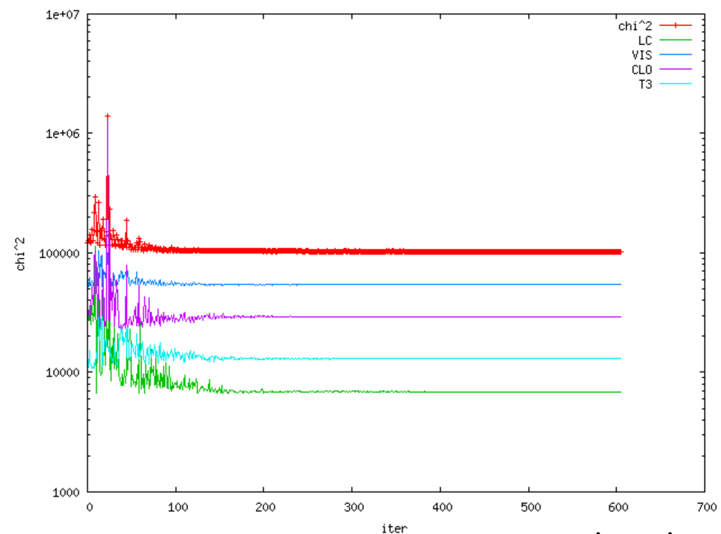

simplex

iteration

Lightcurves (LC)

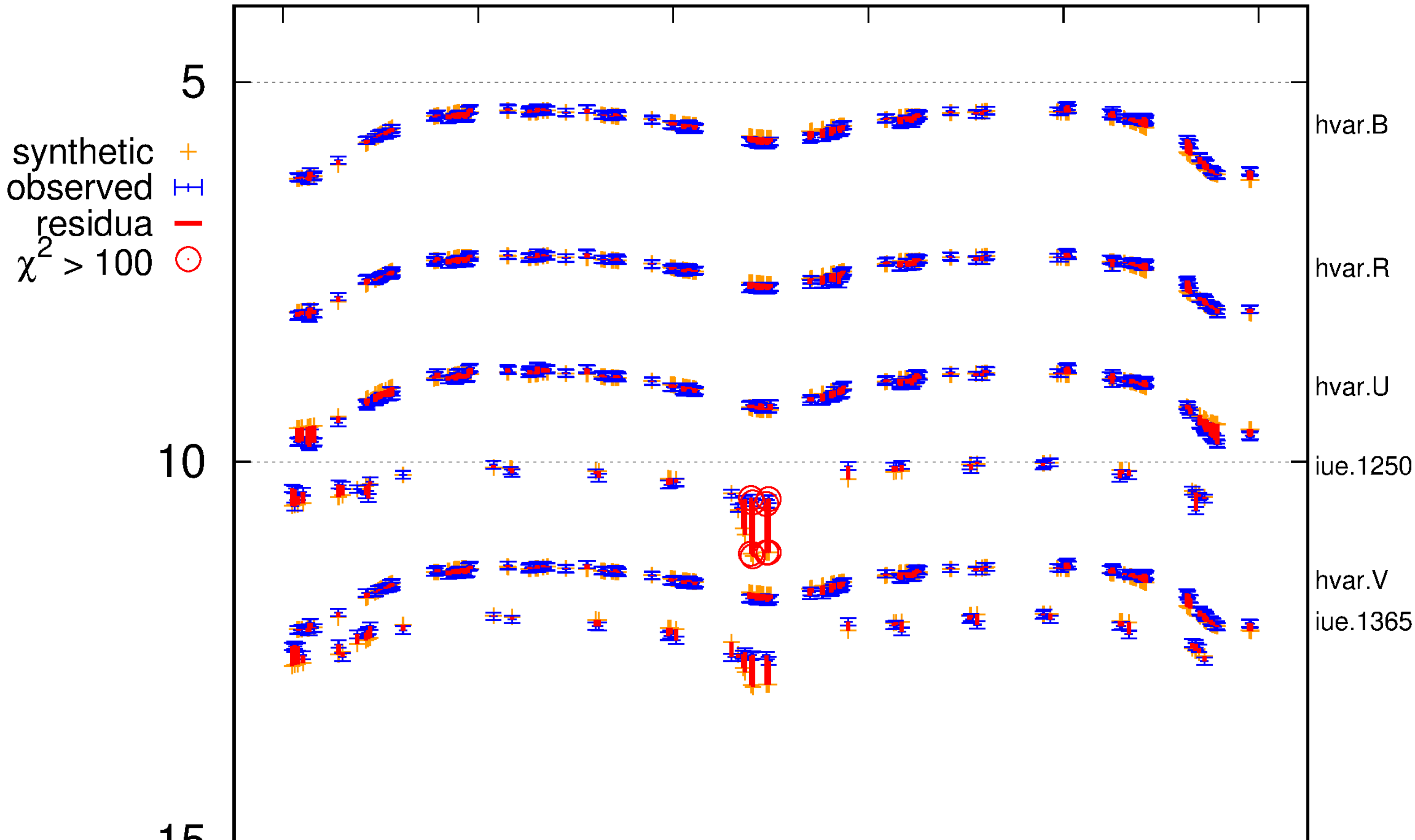

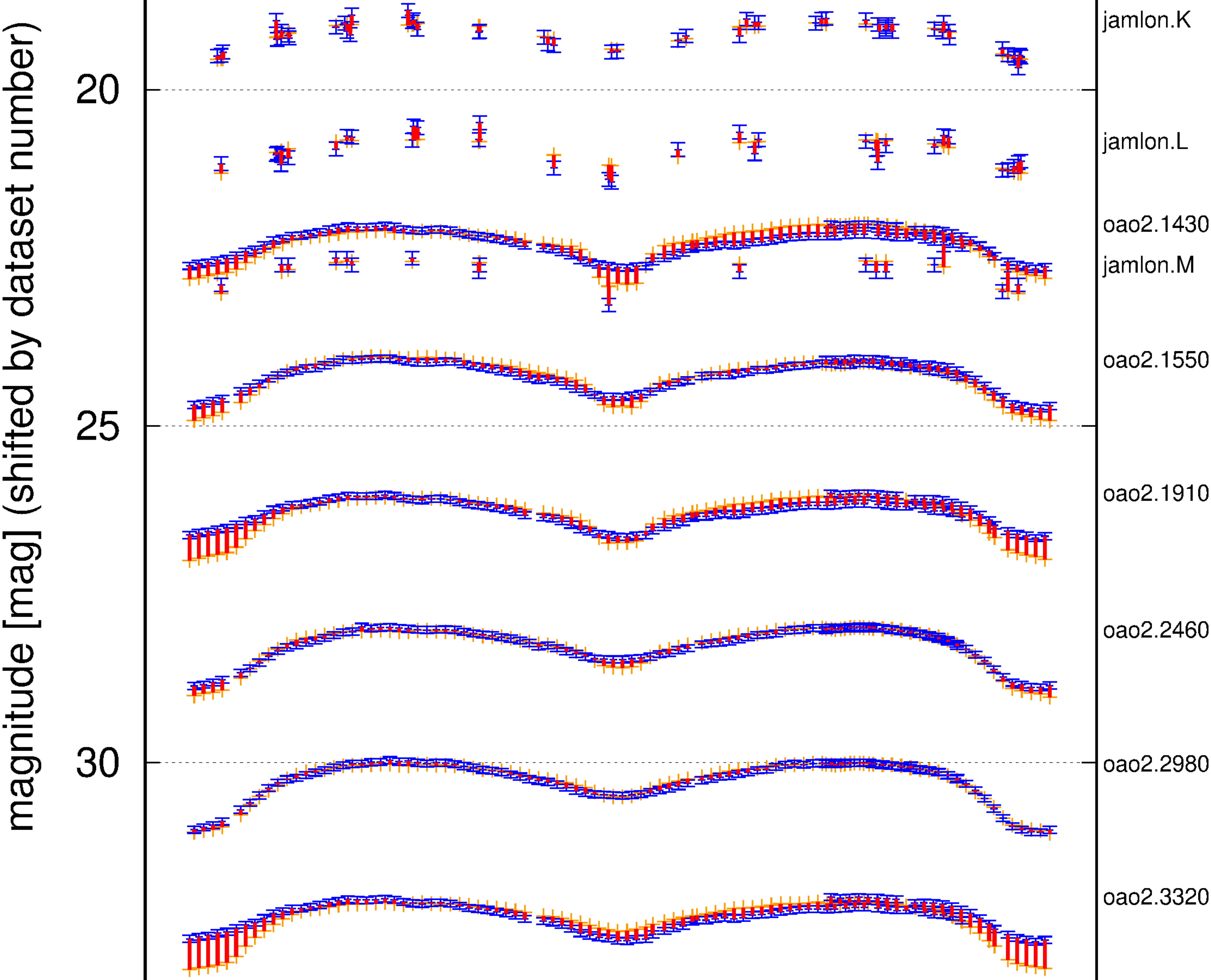

magnitude [mag] (shifted by dataset number)
20
25
30
jamlon.K
jamlon.L
oao2.1430
jamlon.M
oao2.1550
oao2.1910
oao2.2460
oao2.2980
oao2.3320

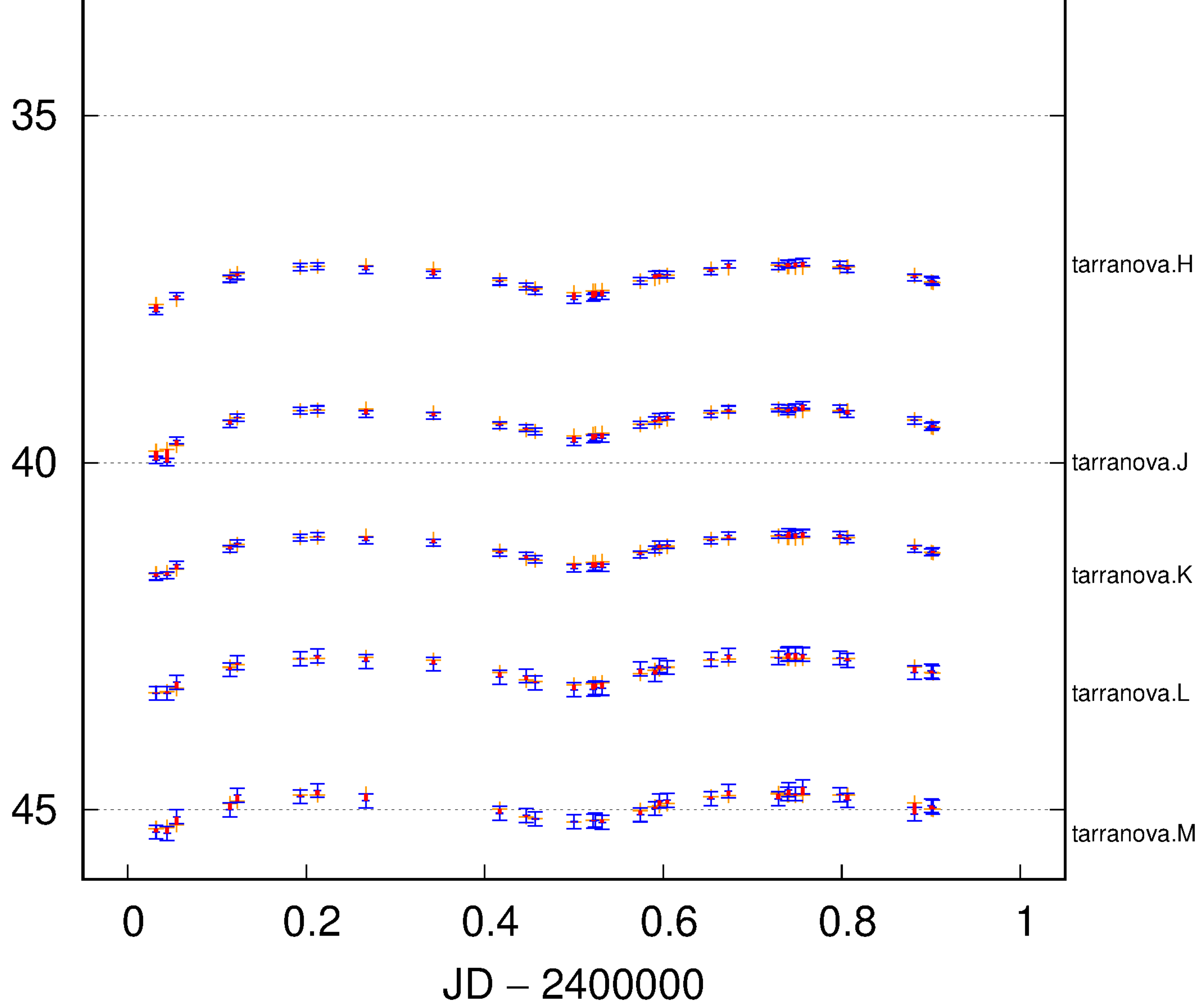
35
40
45
tarranova.H
tarranova.J
tarranova.K
tarranova.L
tarranova.M
0
0.2
0.4
0.6
0.8
1
JD – 2400000

Visibility (VIS)

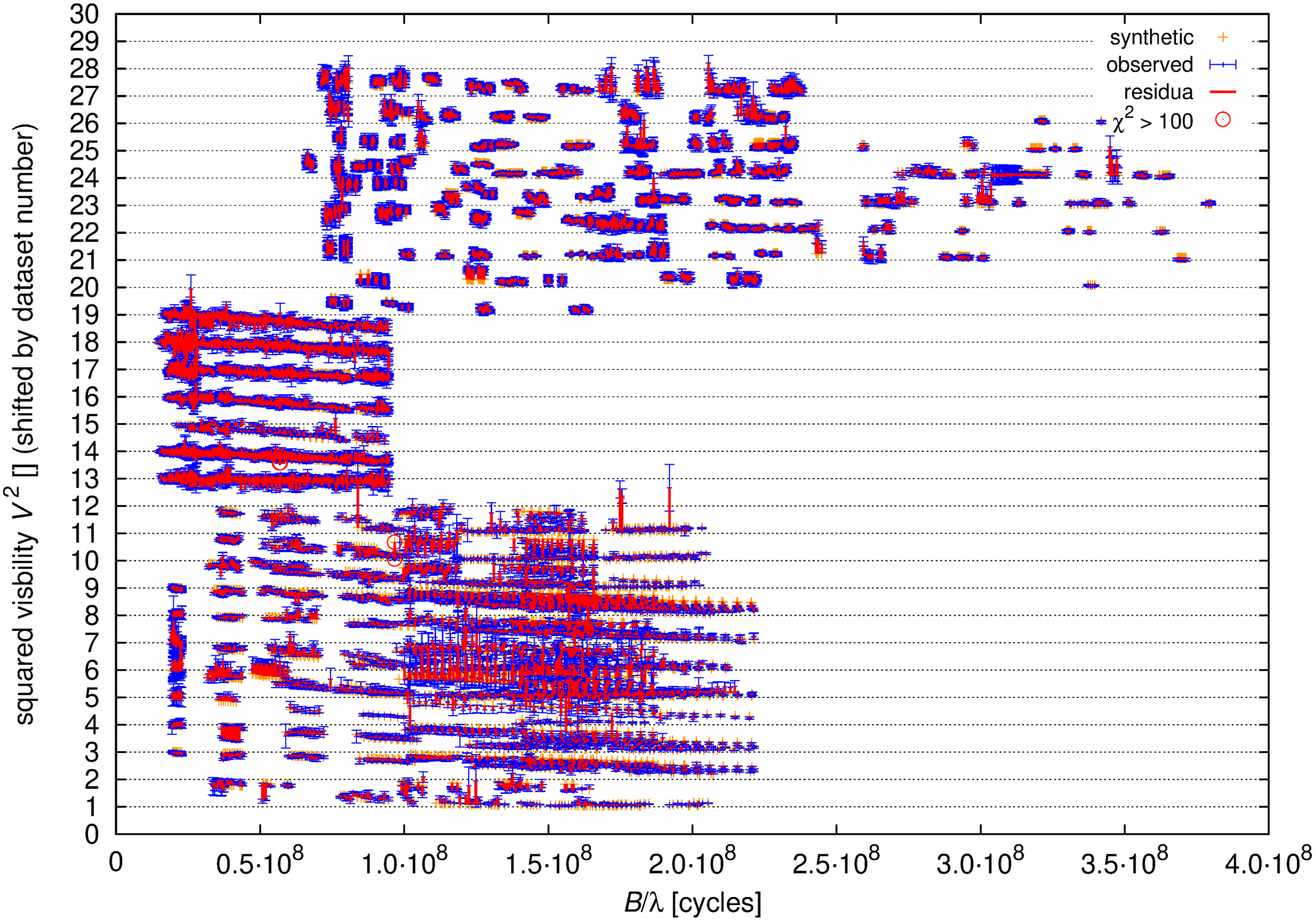

Closure phase (CLO)

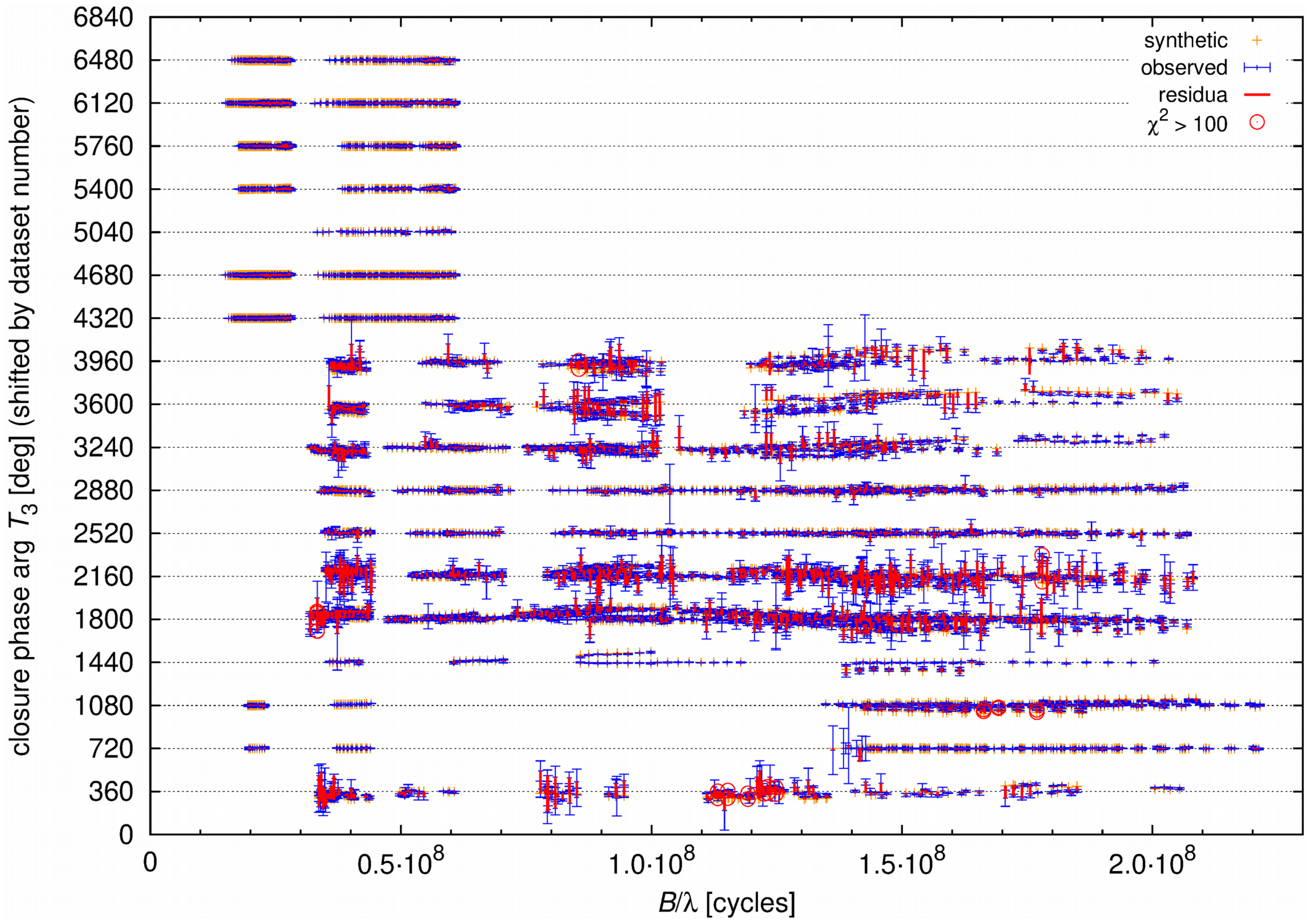

Triple product (T3)

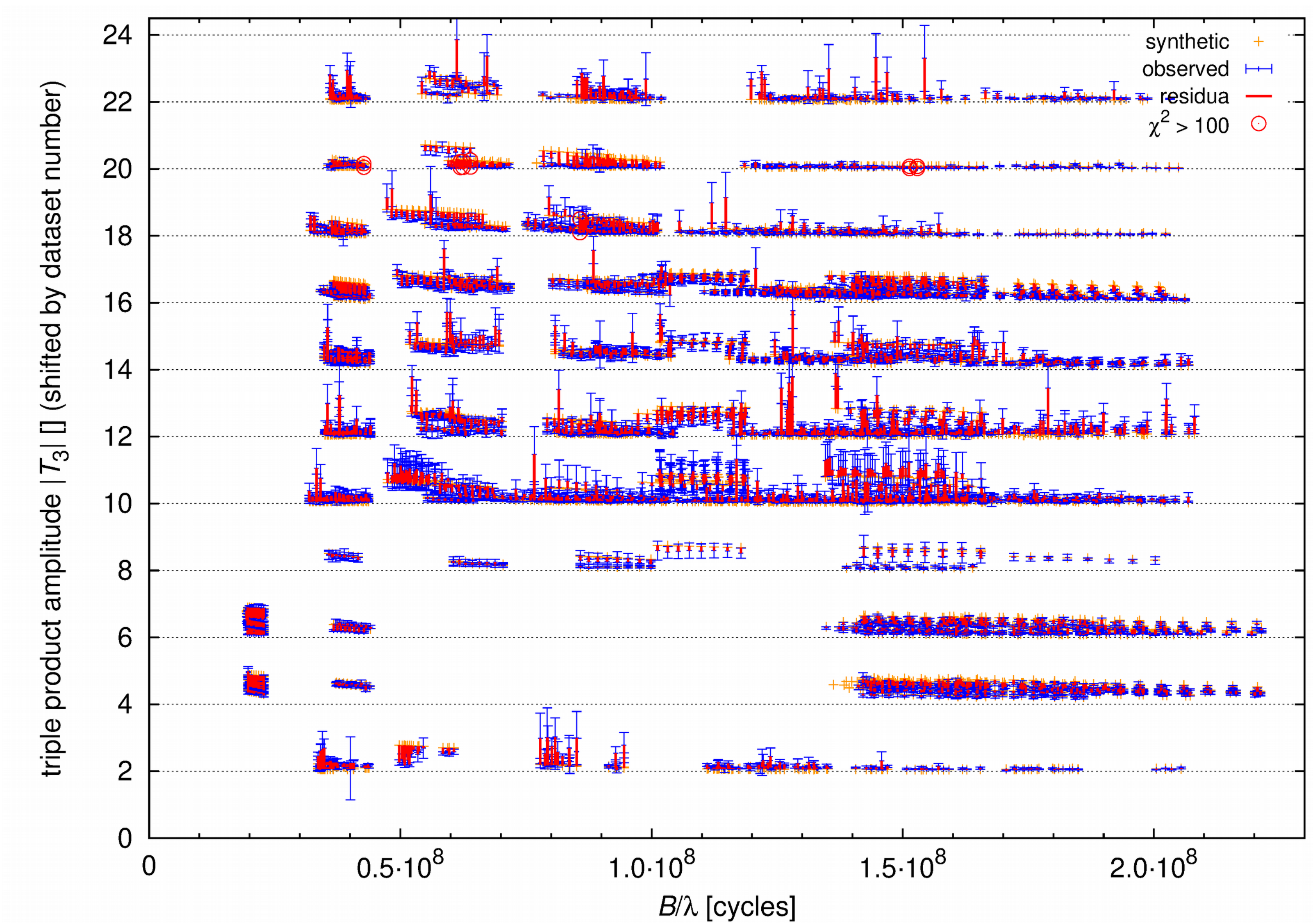

β Lyr A best-fit model

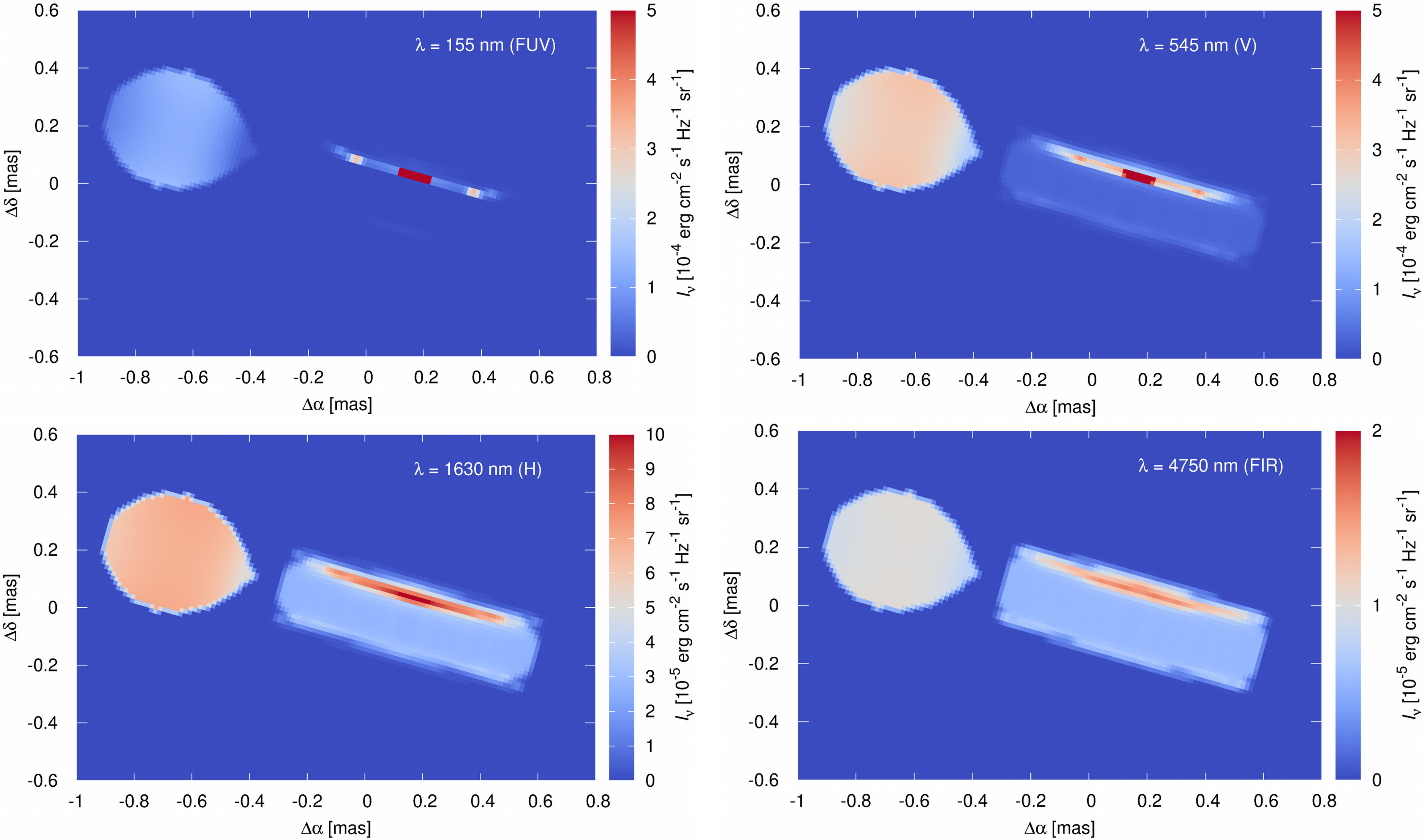

Alternative shapes

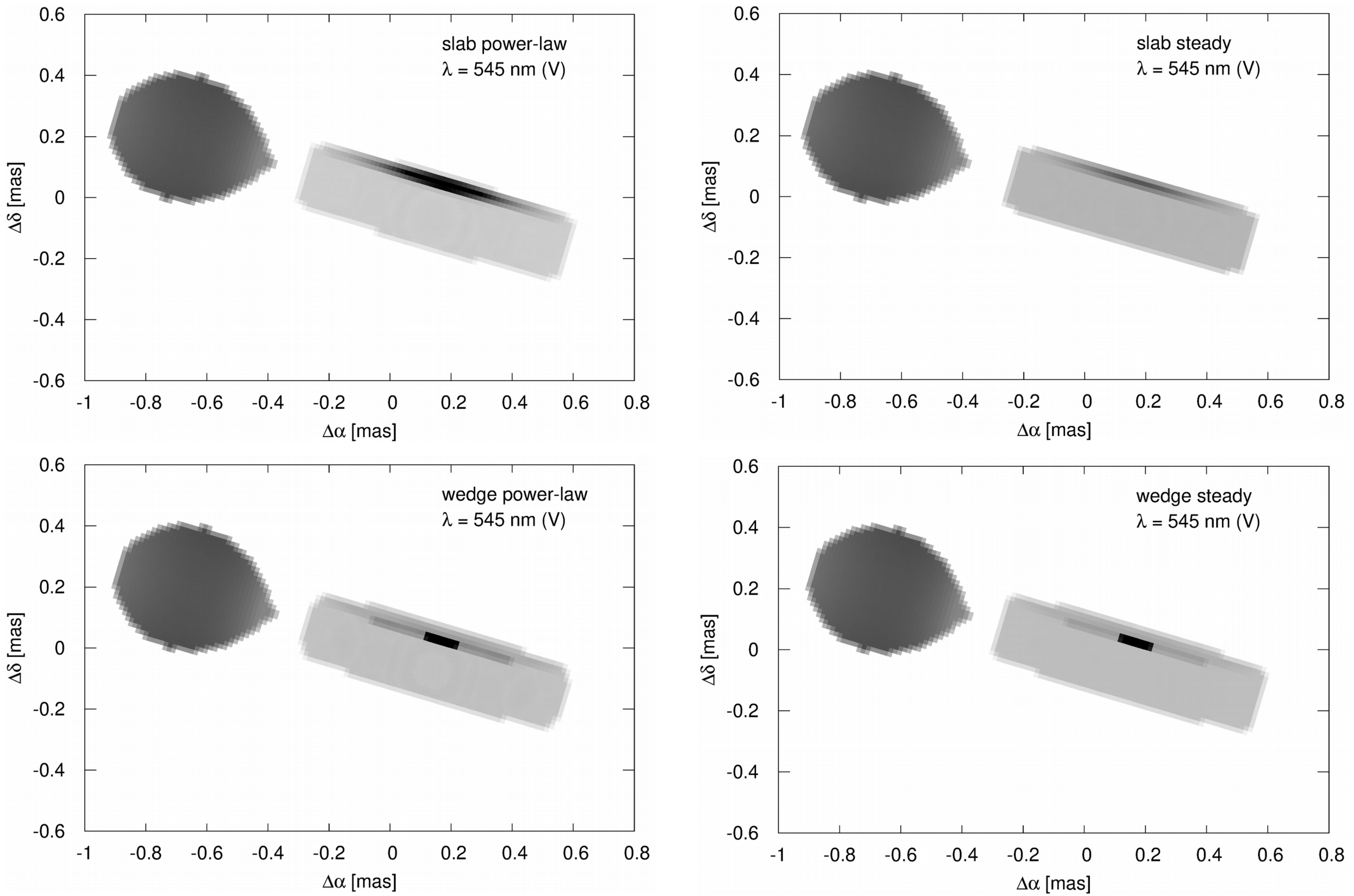

Systematic differences

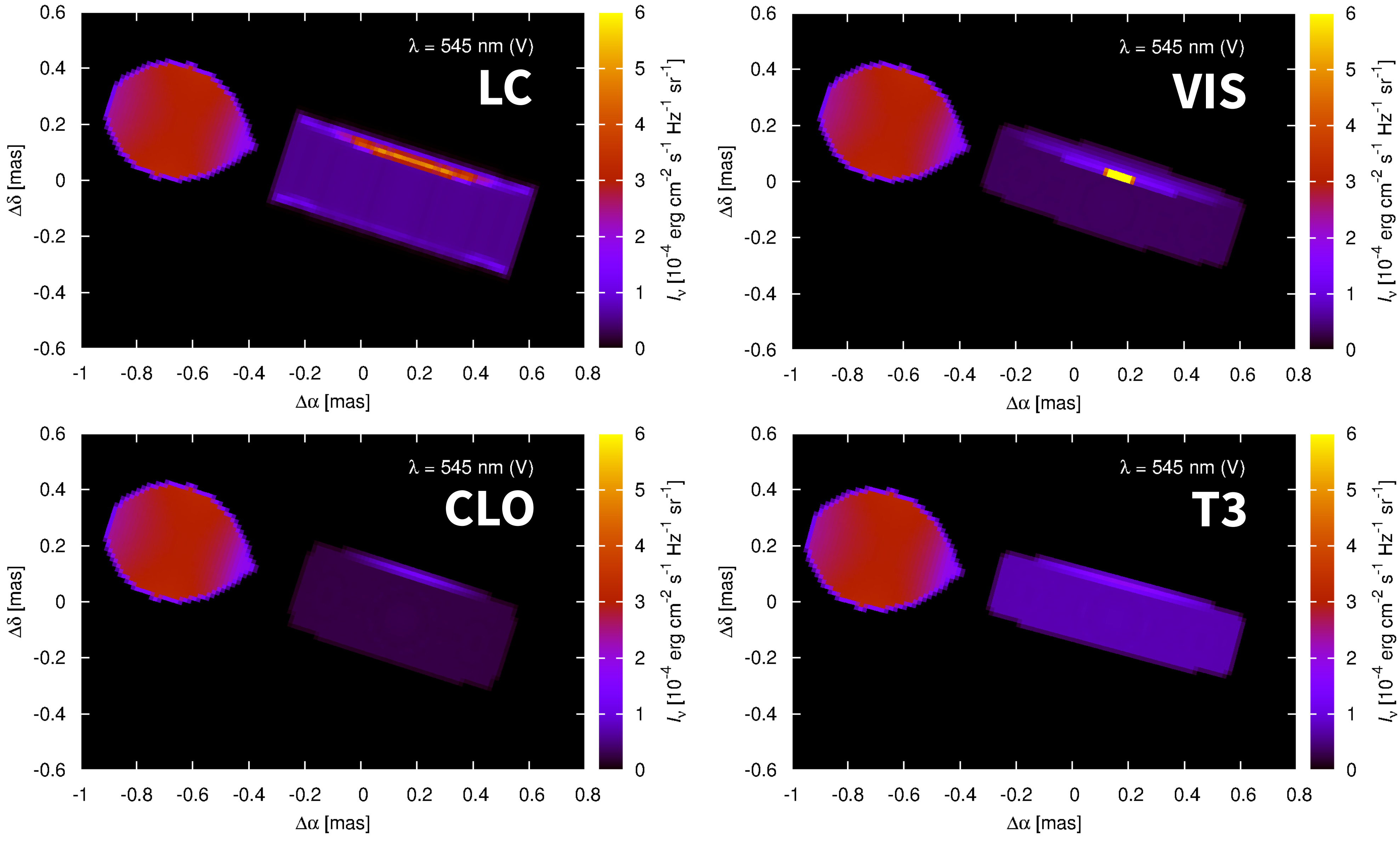

Parameter space

minimum ⟷ maximum

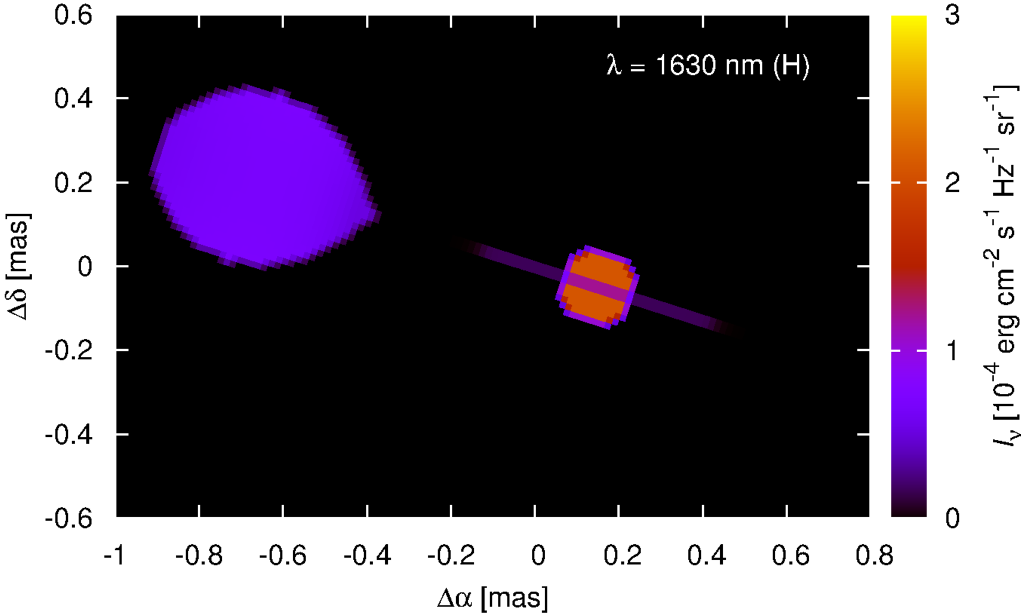

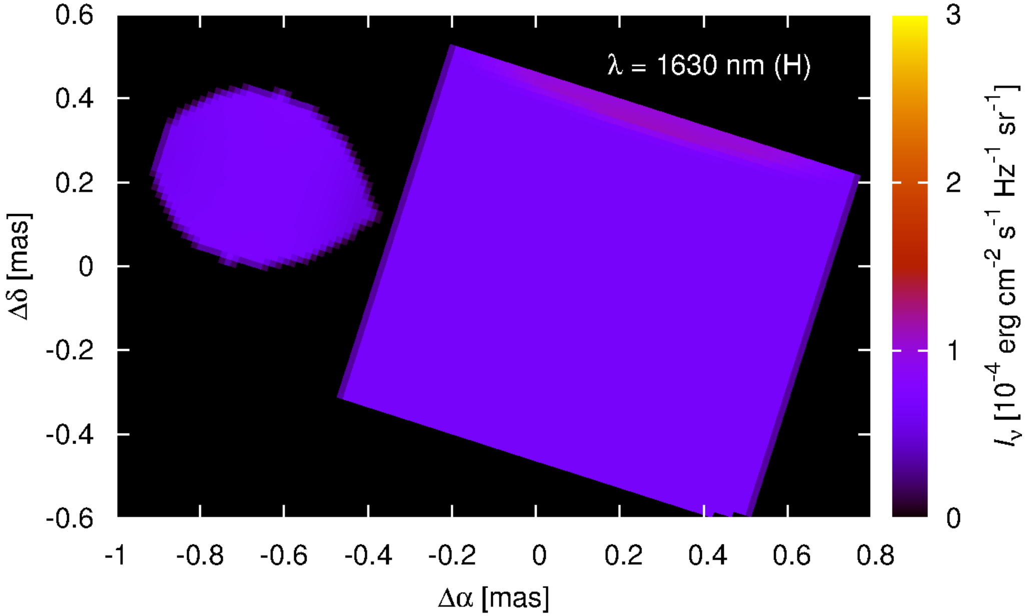

Note: A non-negligible part was explored, but some p. were fixed...

Conclusion: One can be never sure the model is sufficient! (trivial)

Hidden problems

- missing scattering (shadowing), better d. atmosphere
- optically thin jets, spot(s), reflection + irradiation
- limited resolution (~ 1 $R_\odot$), discretisation errors, RTE artifacts
- non-LTE?
- systematics between LC & VIS, CLO, T3
- optically thick vs *very* o. t. ← degenerate problem :(

- missing ΔV^2, Doppler, SED measurements
- kinematics, missing feedback on HD! → dynamical model?
- disk stability, outer edge, precession?

References

Brož & Wolf, Astronomická měření, Praha: Matfyzpress, 2017.

ten Brummelaar et al. (2005), Astrophys. J. **628**, 453

Budaj (2011), Astron. Astrophys. **532**, L12

Chrenko et al. (2017), Astron. Astrophys. **295**, 93

Masset (2000), Astron. Astrophys. Suppl. **141**, 165

Mourard et al. (submitted), Astron. Astrophys.

Rein & Spiegel (2015), Mon. Not. R. Astron. Soc. **446**, 1424